

Signal processing in medical image reconstruction (or: inverse problems in MRI)

Jeffrey A. Fessler

EECS Department
BME Department, Dept. of Radiology
The University of Michigan

EUSIPCO
August 28, 2008

Acknowledgements: Doug Noll, Brad Sutton,
Valur Olafsson, Amanda Funai, Chunyu Yip, Will Grissom

The Broad Perspective

Tour de Sauvabelin

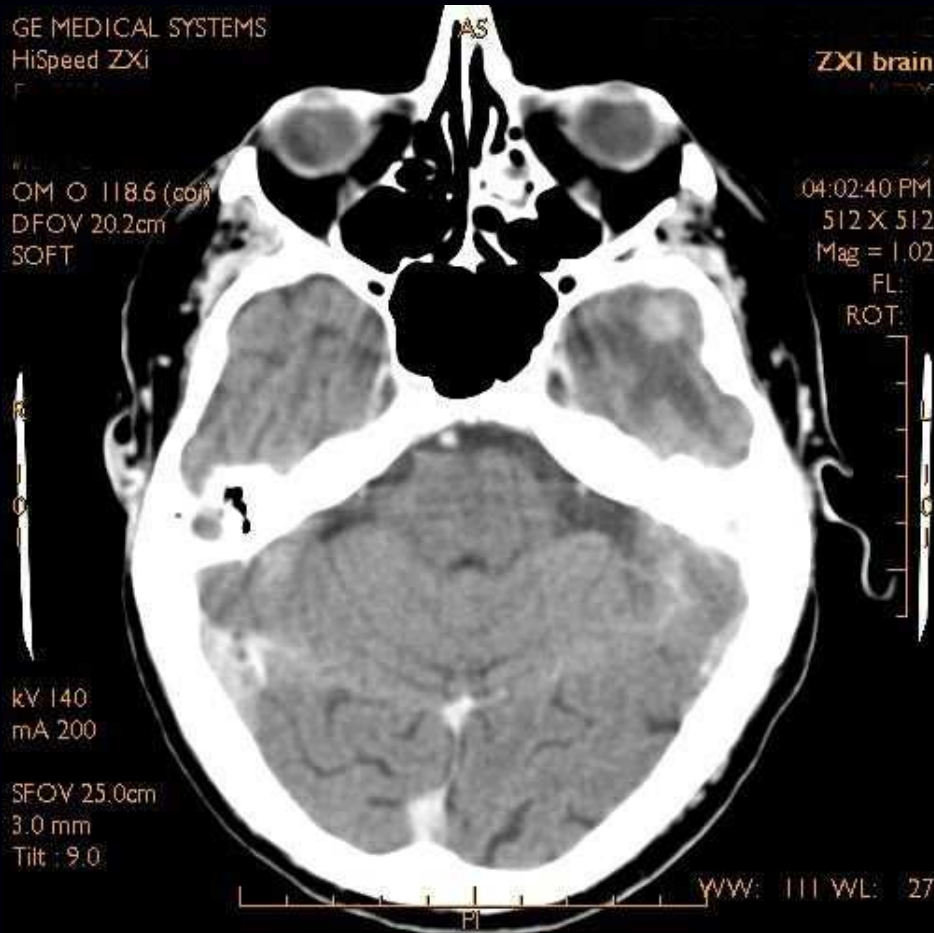
(302 steps to platform at 30m+)

[copyrighted picture]

[copyrighted picture]

<http://www.tour-de-sauvabelin-lausanne.ch>

The Ends



X-ray CT

www.gehealthcare.com



MRI

www.cis.rit.edu

MRI: excellent soft tissue contrast, and no ionizing radiation.
(But, expensive, slow, big, small bone signal...)

Overview

Two inverse problems in MRI

- RF pulse design (spatially selective)
- Image reconstruction
 - Nonuniform fast Fourier transform (NUFFT)
 - Regularization issues (compressed sensing etc.)

Image reconstruction toolbox:

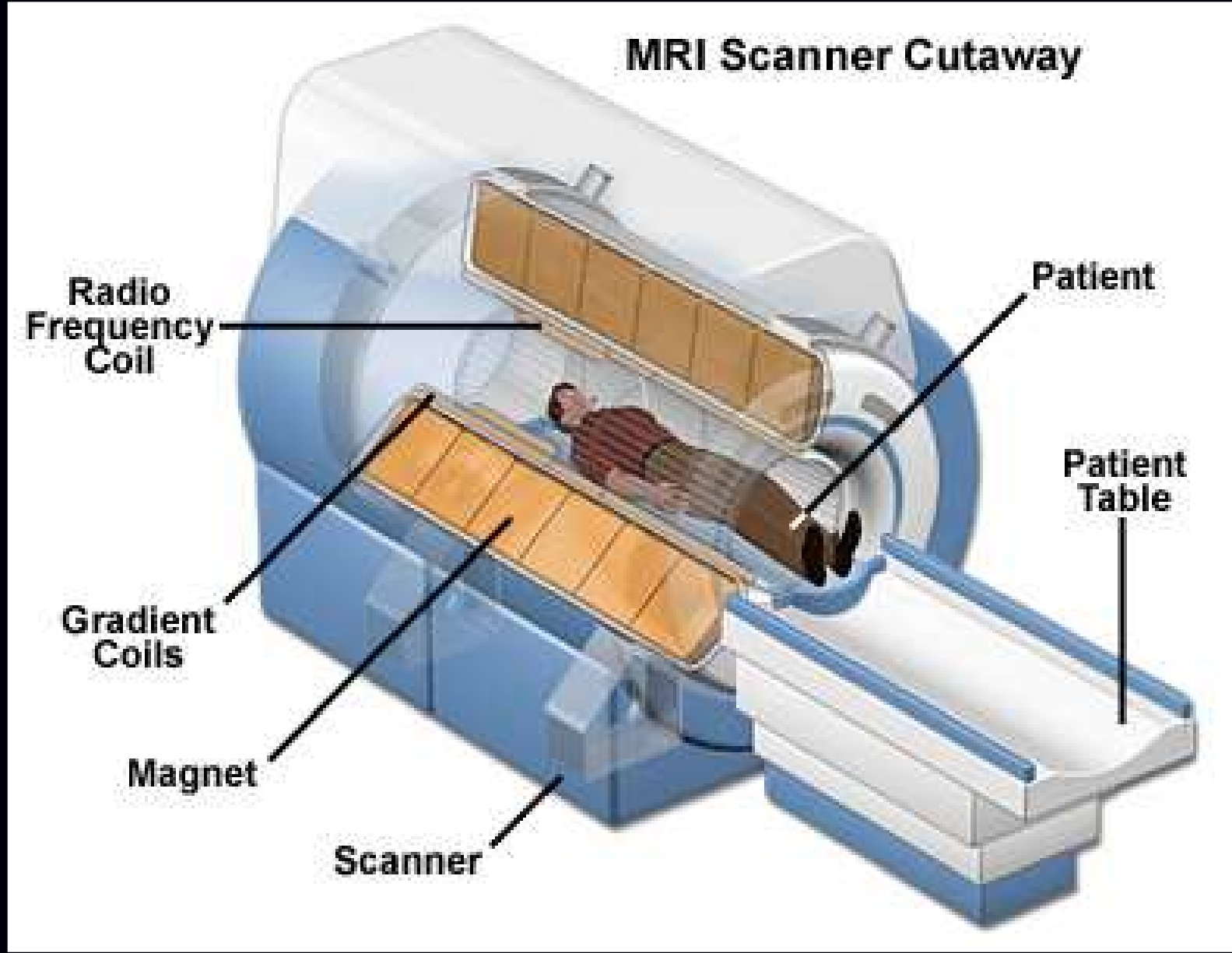
<http://www.eecs.umich.edu/~fessler>

NMR / MRI History (Abbreviated)

- 1946. NMR phenomenon discovered independently by
 - Felix Bloch (Stanford)
 - Edward Purcell (Harvard)
- 1952. Nobel prize in physics to F. Bloch and E. Purcell
- 1966. Richard Ernst and W. Anderson develop Fourier transform spectroscopy
- NMR spectroscopy used in physics and chemistry
- 1971. Ray Damadian discriminates malignant tumors from normal tissue by NMR spectroscopy
- 1973. Paul Lauterbur and Peter Mansfield (independently) add magnetic field gradients, making images
- 1991. Nobel prize in chemistry to R. Ernst for NMR spectroscopy contributions
- 2002. Nobel prize in chemistry to Kurt Wüthrich for using NMR spectroscopy to determine 3D structure of biological macromolecules in solution
- 2003. Nobel prize in medicine to P. Lauterbur and Sir P. Mansfield!
- 2005. Researchers apply compressed sensing / sparsity ideas to MRI
Medical imaging conferences very dense with related papers since...

Physics

MRI Scanner



www.magnet.fsu.edu

Bloch Equation - Overview

PHYSICAL REVIEW

VOLUME 70, NUMBERS 7 AND 8

OCTOBER 1 AND 15, 1946

Nuclear Induction

F. BLOCH

Stanford University, California

Nuclei with odd number of protons or neutrons (e.g., ^1H) have *nuclear spin angular momentum*. These magnetic moments tend to align with an applied magnetic field, and collectively the spins induce local magnetization.

The (phenomenological) Bloch Equation describes the time evolution of local magnetization $\mathbf{M}(\mathbf{r}, t)$:

$$\frac{d\mathbf{M}}{dt} = \mathbf{M} \times \gamma \mathbf{B} - \frac{M_x \mathbf{i} + M_y \mathbf{j}}{T_2} - \frac{(M_z - M_0) \mathbf{k}}{T_1}$$

Precession
Relaxation
Equilibrium



Bloch Equation and Imaging

$$\frac{d\mathbf{M}(\mathbf{r},t)}{dt} = \mathbf{M}(\mathbf{r},t) \times \gamma \mathbf{B}(\mathbf{r},t) - \frac{M_x \mathbf{i} + M_y \mathbf{j}}{T_2(\mathbf{r})} - \frac{(M_z - M_0(\mathbf{r})) \mathbf{k}}{T_1(\mathbf{r})}$$

Image properties depend on:

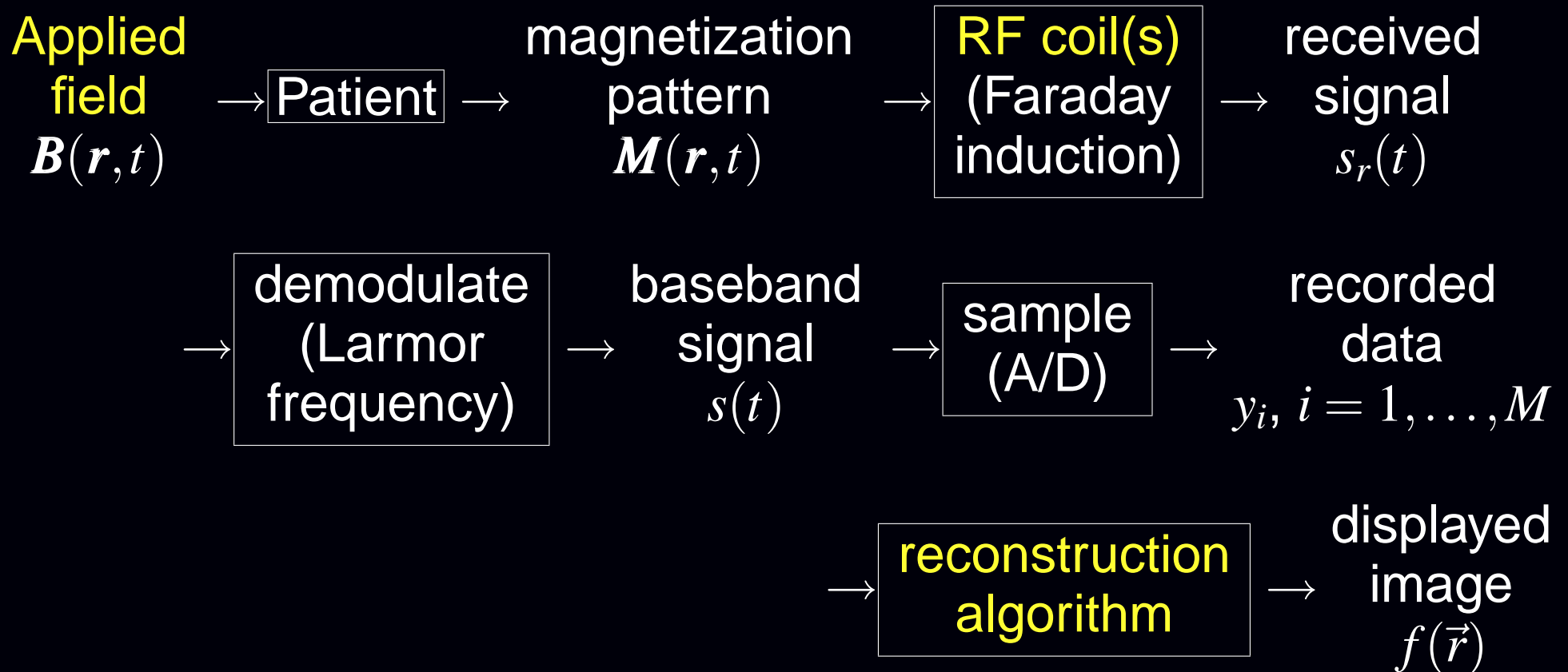
- Steady-state magnetization $M_0(\mathbf{r}) \propto$ spin (Hydrogen) density
- Longitudinal (spin-lattice) relaxation $T_1(\mathbf{r})$
- Transverse (spin-spin) relaxation $T_2(\mathbf{r})$
- Chemical shift
(resonant frequency of H is ≈ 3.5 ppm lower in fat than in water)

Applied field $\mathbf{B}(\mathbf{r},t)$ includes three components we can control:

- Main field B_0 (static)
- RF field $\mathbf{B}_1(t)$
- Field gradients $\mathbf{r} \cdot \mathbf{G}(t) = xG_x(t) + yG_y(t) + zG_z(t)$

$$\mathbf{B}(\mathbf{r},t) = B_0 + \mathbf{B}_1(t) + \mathbf{r} \cdot \mathbf{G}(t) \mathbf{k}$$

Systems view of MRI



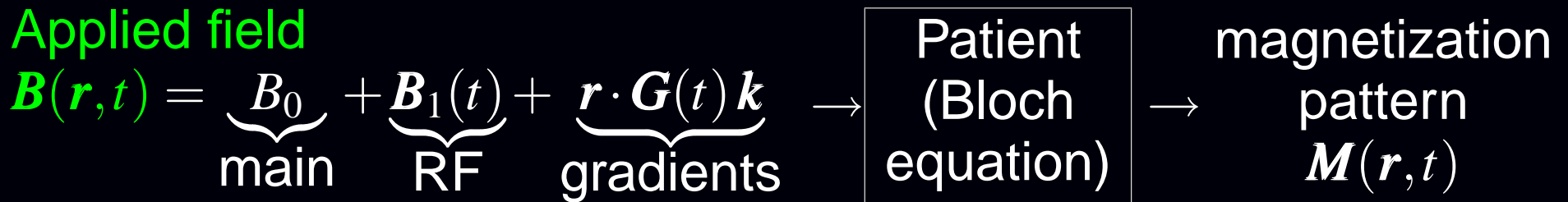
Research areas:

- **design of RF pulses** / gradient waveforms (*many possibilities!*)
- coil design
- contrast agents
- **reconstruction algorithm development** / data processing

**Inverse Problem 1:
RF Pulse Design
for “Excitation”**

RF Pulse Design: Forward Model

Forward model:



Rewriting Bloch equation:

$$\frac{d}{dt} \mathbf{M}(\mathbf{r}, t) = \mathbf{M}(\mathbf{r}, t) \times \gamma \mathbf{B}(\mathbf{r}, t) - \mathbf{T} [\mathbf{M}(\mathbf{r}, t) - \mathbf{M}(\mathbf{r}, 0)]$$

where $\mathbf{T} = \begin{bmatrix} 1/T_2(\mathbf{r}) & 0 & 0 \\ 0 & 1/T_2(\mathbf{r}) & 0 \\ 0 & 0 & 1/T_1(\mathbf{r}) \end{bmatrix}$.

RF pulse design goals: find RF waveform $B_1(t)$, $0 \leq t \leq t_1$ that induces some desired magnetization pattern $\mathbf{M}_d(\mathbf{r}, t_1)$ at pulse end. This is a “noiseless” inverse problem.

RF Pulse Design: Inverse Problem

Problem is typically over-determined, so apply LS approach:

$$\arg \min_{\{B_1(n\Delta_t)\}} \sum_{\mathbf{r}} |\mathbf{M}(\mathbf{r}, t_1) - \mathbf{M}_d(\mathbf{r}, t_1)|^2$$

subject to constraints:

- RF amplitude, bandwidth (hardware)
- RF power deposition (patient safety)

Challenge: no general solution to Bloch equation

⇒ forward model requires numerical methods

⇒ inverse problem slow (fine grid sampling in \mathbf{r})

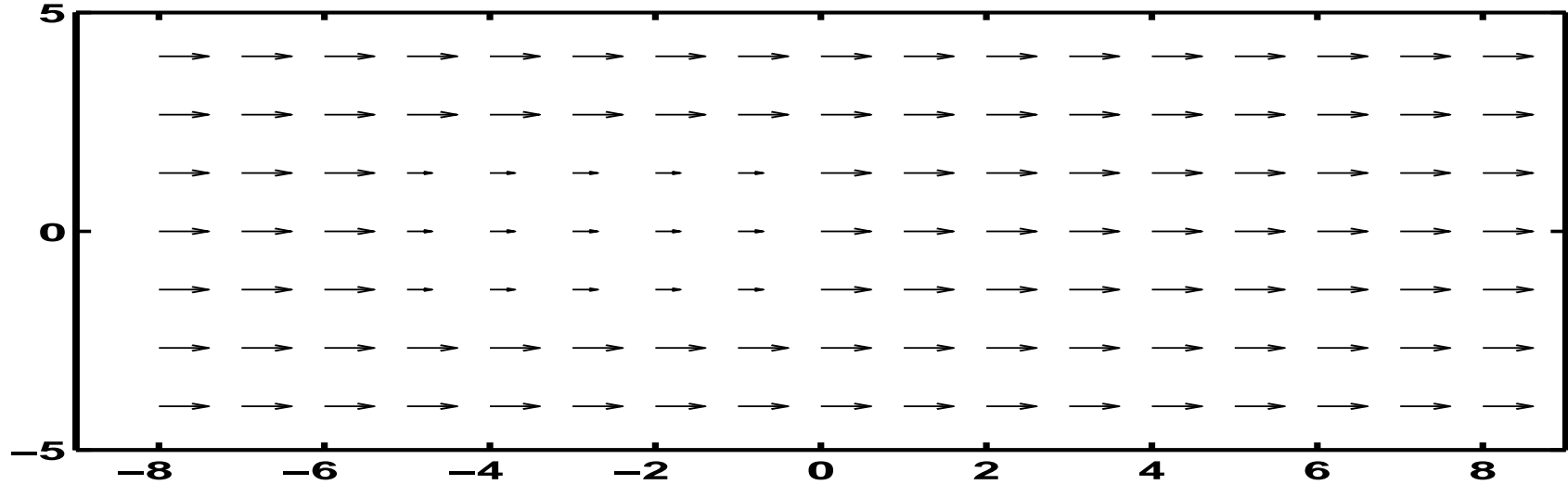
RF Excitation: Applications

(Exciting all spins is relatively easy, *cf.* NMR spectroscopy)

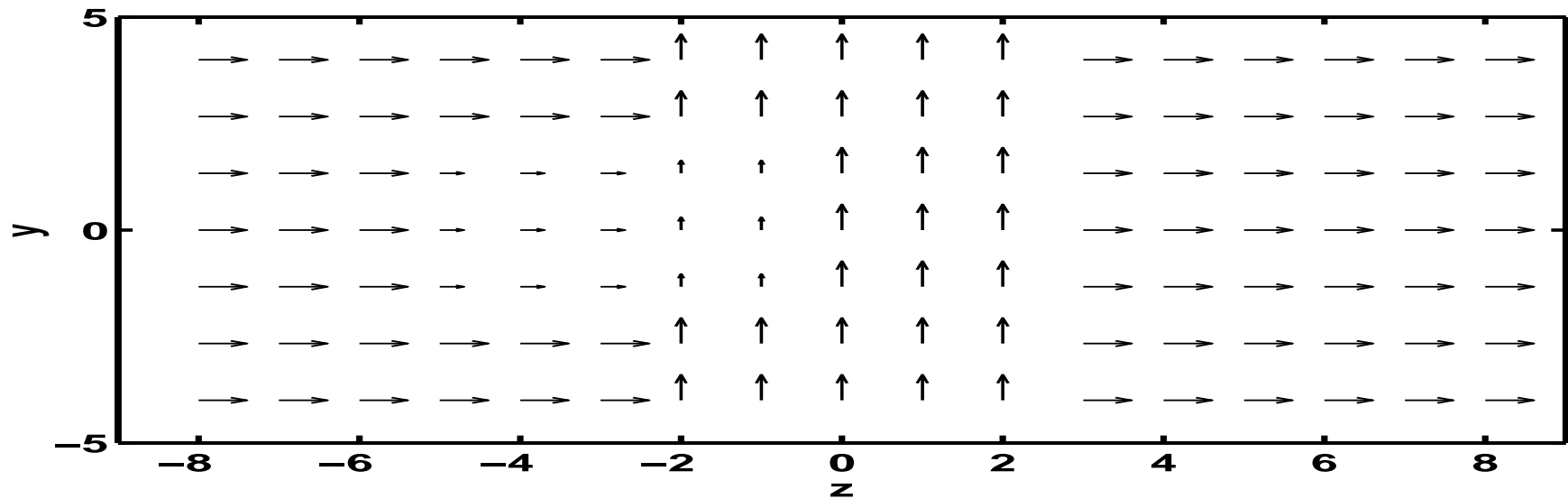
- slice selection (1D)
- spatially selective excitation (2D and 3D)
 - imaging small regions
 - compensating for undesired spin phase evolution (fMRI)
 - compensating for nonuniform coil sensitivity (high field)

RF Excitation: Slice Selection

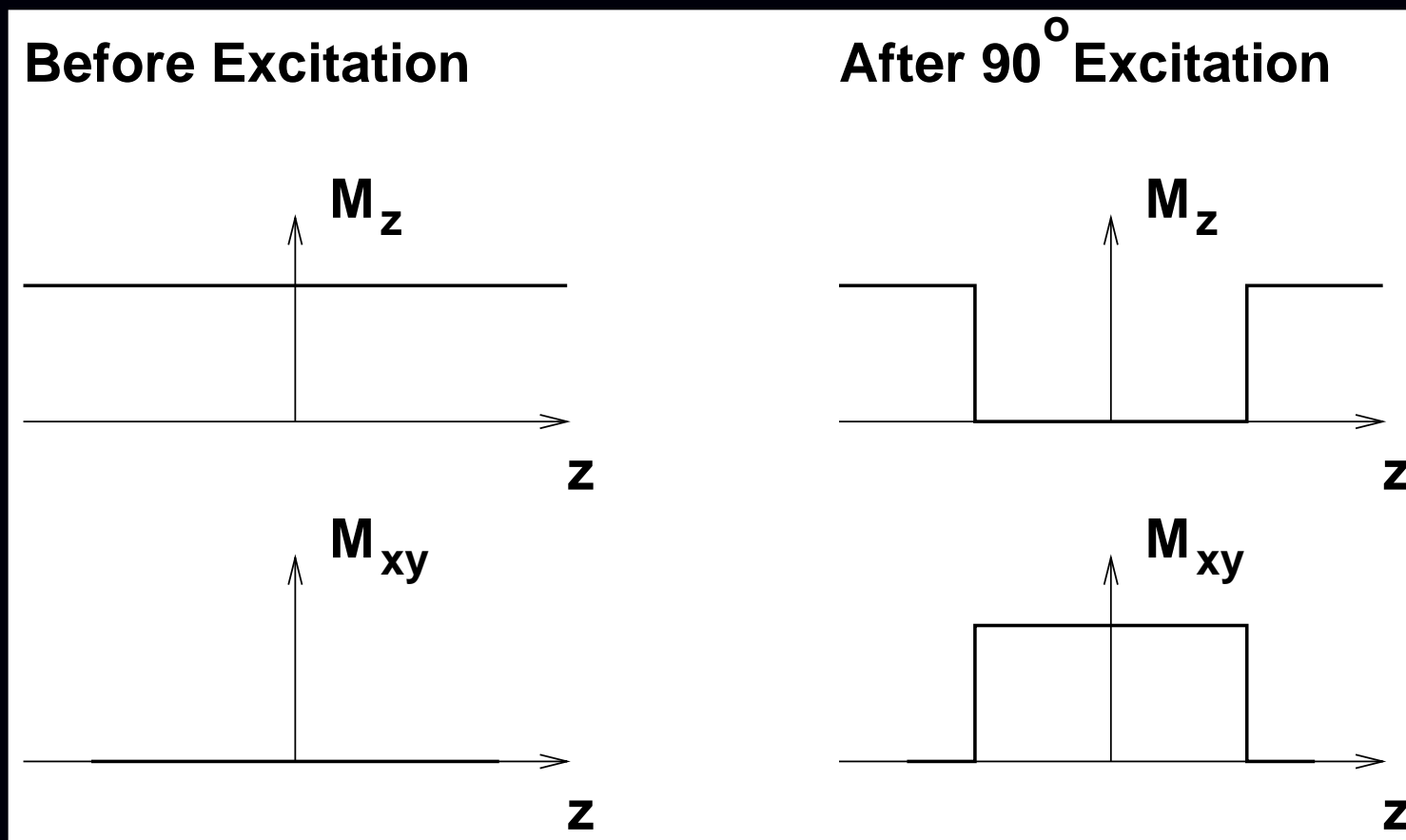
Before Excitation (Equilibrium)



After Ideal Slab Excitation



RF Excitation: Slice Selection

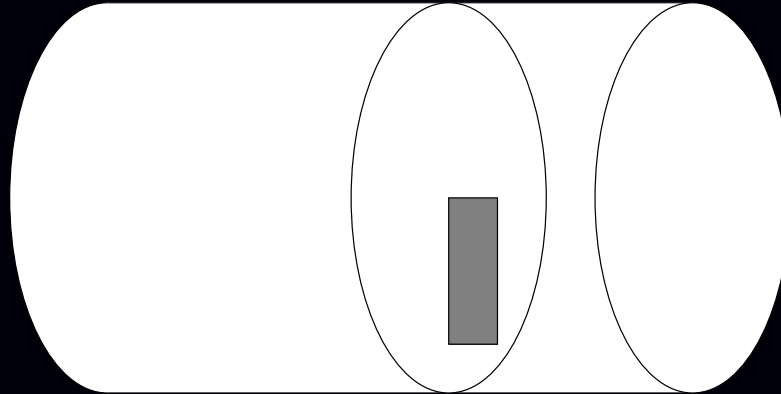


Here, forward model simplifies to (roughly speaking) a Fourier transform relationship between RF pulse $B_1(t)$ and slice profile.

Practical RF design methods exist. (Pauly *et al.*, IEEE T-MI, Mar. 1991)
(Uses Parks-McClellan FIR filter design technique.)

RF Excitation: Spatially Selective

Excite only spins within some region of interest

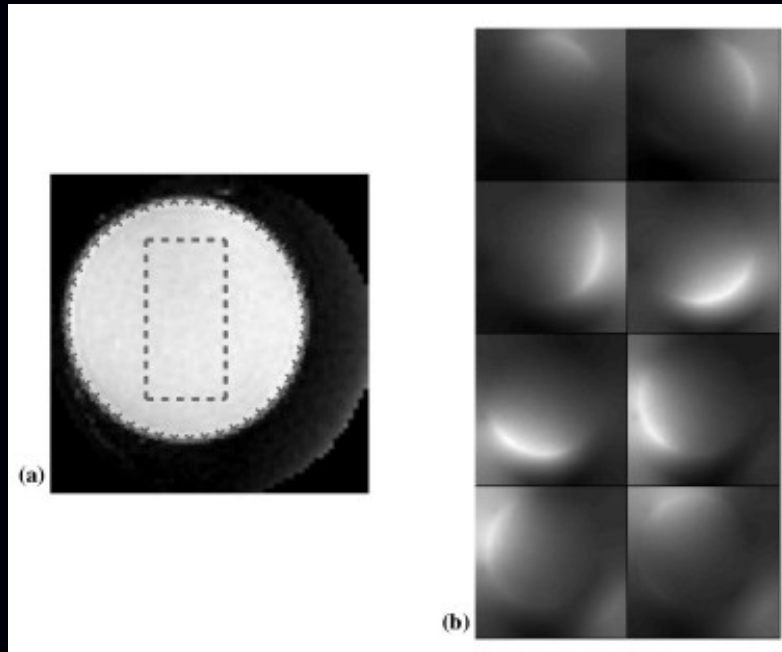


Challenges:

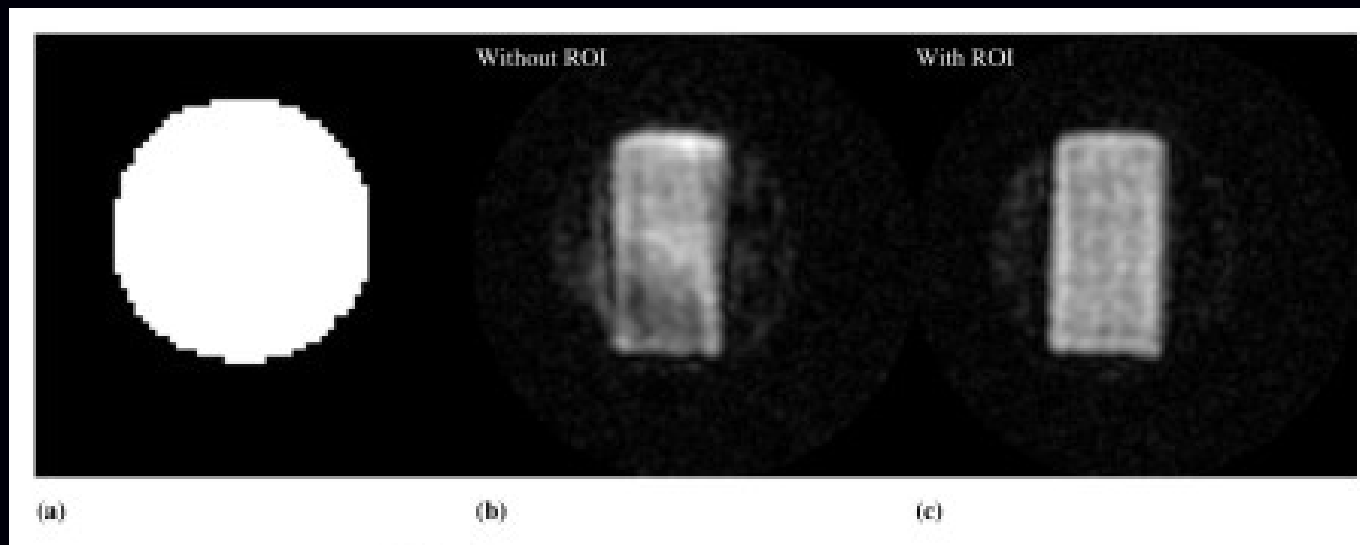
- Computation
- Magnetic field inhomogeneity
- Coil field pattern nonuniformity
- Multiple coils
- Joint design of RF pulse $B_1(t)$ and gradient waveforms $\mathbf{G}(t)$

This is an active research area.

Multiple-coil RF Pulse Design Example

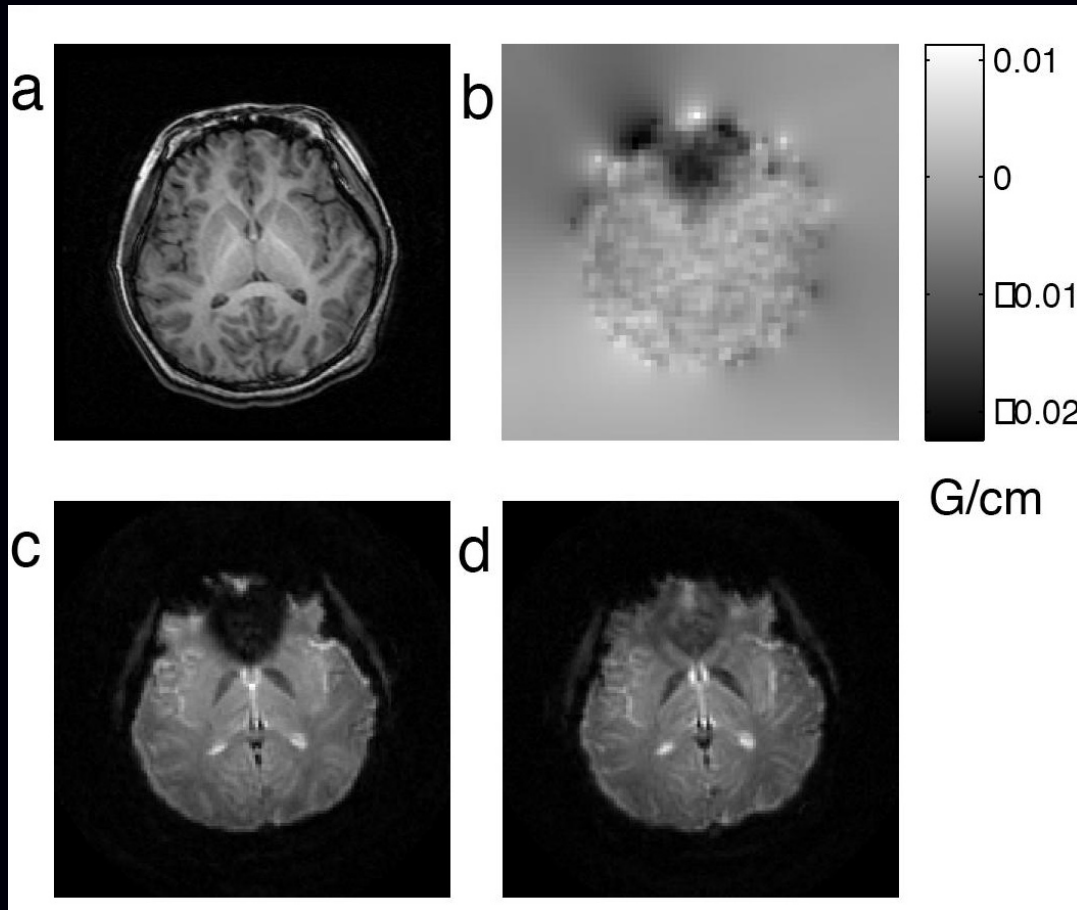


Grissom *et al.*, MRM, Sep. 2006
Approach: linearization,
nonuniform FFT, iterative CG



Example: Iterative RF Pulse Design

Tailored RF pulses for through-plane dephasing compensation

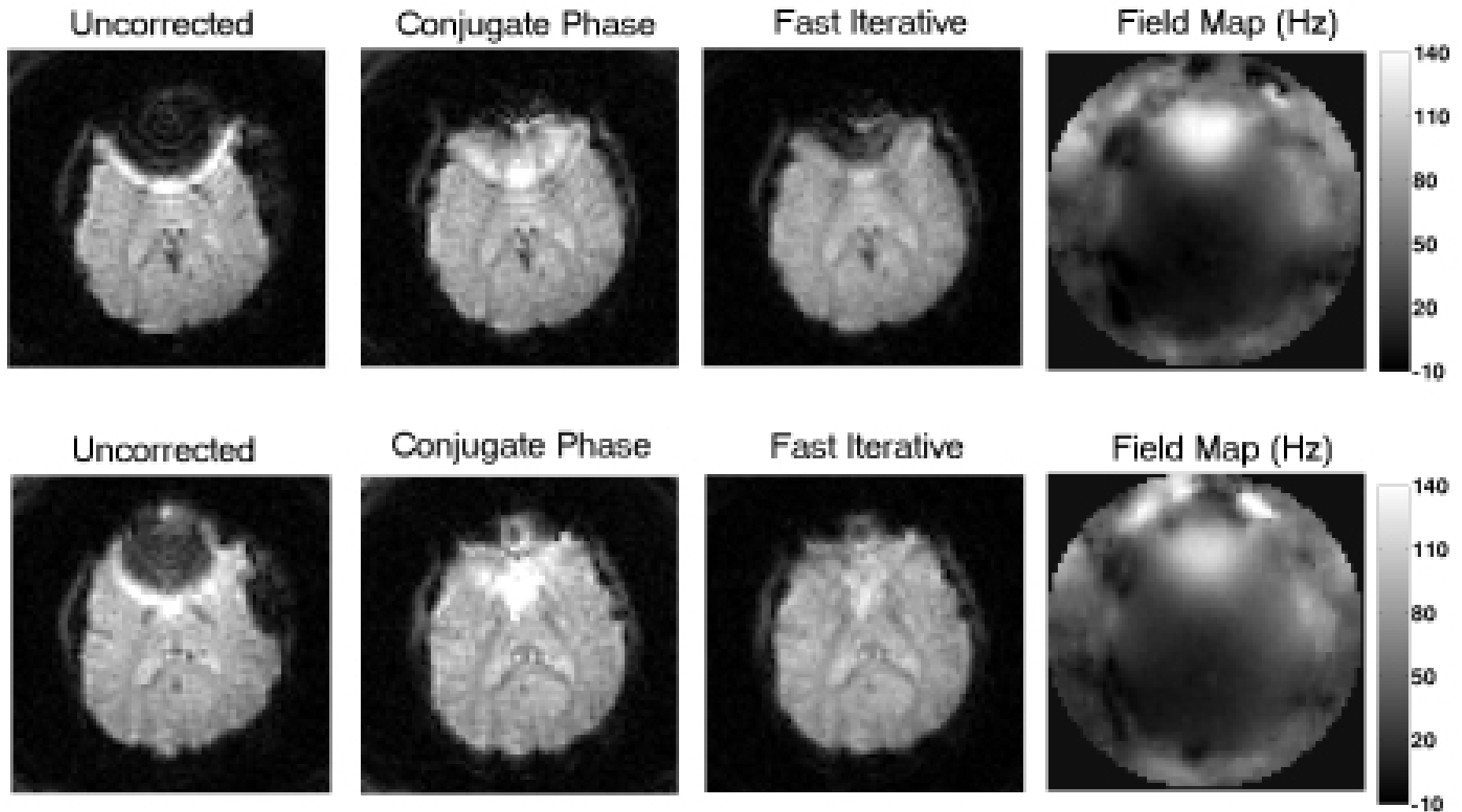


Yip *et al.*, MRM, Nov. 2006
Uses fast- k_z excitation k-space trajectory with a few k_x, k_y phase encodes.

Challenges: patient specific, requiring “on line” computation, design of excitation k-space trajectory.

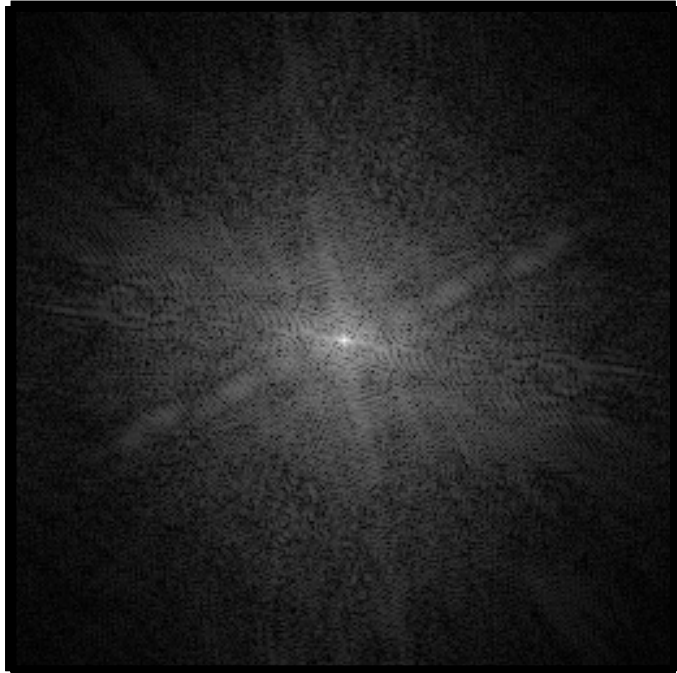
Inverse Problem 2: MR Image Reconstruction

Example: Iterative Reconstruction under ΔB_0



Standard MR Image Reconstruction

MR k-space data Reconstructed Image



Cartesian sampling in k-space. An inverse FFT. End of story.

Commercial MR system quotes 400 FFTs (256^2) per second.

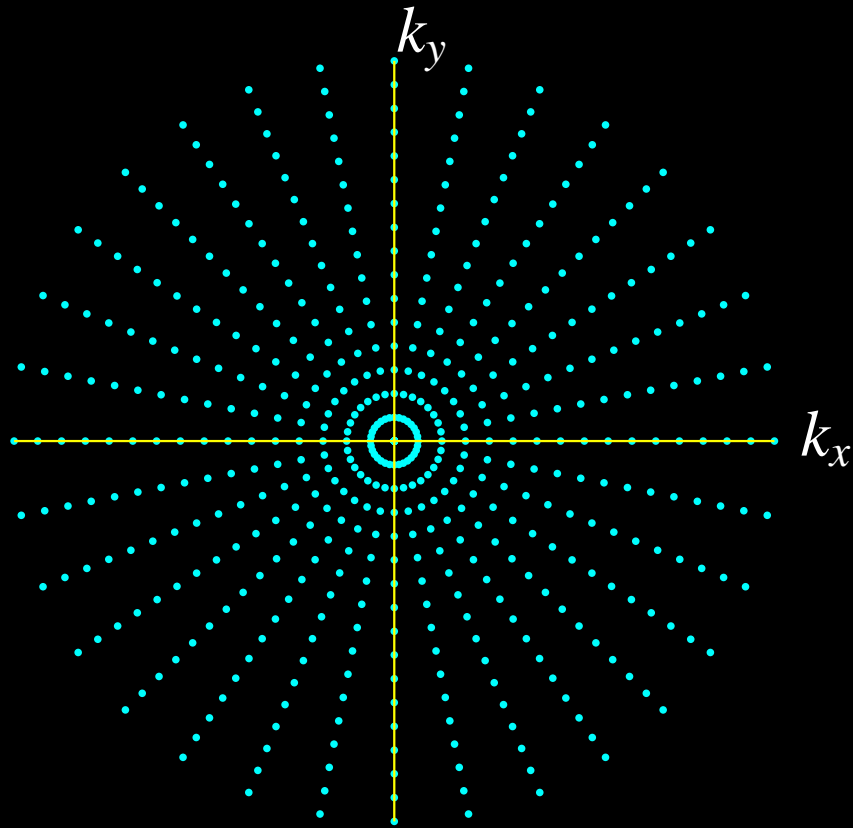
Non-Cartesian MR Image Reconstruction

“k-space” data

$$\mathbf{y} = (y_1, \dots, y_M)$$

image

$$f(\vec{r})$$



k-space trajectory:

$$\vec{\mathbf{k}}(t) = (k_x(t), k_y(t))$$



spatial coordinates:

$$\vec{r} \in \mathbb{R}^d$$

Textbook MRI Measurement Model

Ignoring *lots* of things, the standard measurement model is:

$$y_i = s(t_i) + \text{noise}_i, \quad i = 1, \dots, M$$
$$s(t) = \int f(\vec{r}) e^{-i2\pi\vec{k}(t)\cdot\vec{r}} d\vec{r} = F(\vec{k}(t)).$$

\vec{r} : spatial coordinates

$\vec{k}(t)$: k-space trajectory of the MR pulse sequence

$f(\vec{r})$: object's unknown **transverse magnetization**

$F(\vec{k})$: Fourier transform of $f(\vec{r})$. We get noisy samples of this!

$e^{-i2\pi\vec{k}(t)\cdot\vec{r}}$ provides spatial information \implies Nobel Prize

Goal of image reconstruction: find $f(\vec{r})$ from measurements $\{y_i\}_{i=1}^M$.

The unknown object $f(\vec{r})$ is a continuous-space function, but the recorded measurements $\mathbf{y} = (y_1, \dots, y_M)$ are finite.

Under-determined (ill posed) problem \implies no canonical solution.

All MR scans provide only “partial” k-space data.

Image Reconstruction Strategies

- Continuous-continuous formulation

Pretend that a continuum of measurements are available:

$$F(\vec{\mathbf{k}}) = \int f(\vec{\mathbf{r}}) e^{-i2\pi\vec{\mathbf{k}}\cdot\vec{\mathbf{r}}} d\vec{\mathbf{r}}.$$

The “solution” is an inverse Fourier transform:

$$f(\vec{\mathbf{r}}) = \int F(\vec{\mathbf{k}}) e^{i2\pi\vec{\mathbf{k}}\cdot\vec{\mathbf{r}}} d\vec{\mathbf{k}}.$$

Now discretize the integral solution:

$$\hat{f}(\vec{\mathbf{r}}) = \sum_{i=1}^M F(\vec{\mathbf{k}}_i) e^{i2\pi\vec{\mathbf{k}}_i\cdot\vec{\mathbf{r}}} w_i \approx \sum_{i=1}^M y_i w_i e^{i2\pi\vec{\mathbf{k}}_i\cdot\vec{\mathbf{r}}},$$

where w_i values are “sampling density compensation factors.” Numerous methods for choosing w_i values in the literature.

For Cartesian sampling, using $w_i = 1/N$ suffices, and the summation is an inverse FFT.

For non-Cartesian sampling, replace summation with **gridding**.

- Continuous-discrete formulation

Use many-to-one linear model:

$$\mathbf{y} = \mathcal{A} f + \boldsymbol{\varepsilon}, \text{ where } \mathcal{A} : \mathcal{L}_2(\mathbb{R}^{\bar{d}}) \rightarrow \mathbb{C}^M.$$

Minimum norm solution (cf. “natural pixels”):

$$\min_{\hat{f}} \|\hat{f}\|_2 \text{ subject to } \mathbf{y} = \mathcal{A} \hat{f}$$

$$\hat{f} = \mathcal{A}^* (\mathcal{A} \mathcal{A}^*)^{-1} \mathbf{y} = \sum_{i=1}^M c_i e^{-i2\pi \vec{\mathbf{k}}_i \cdot \vec{\mathbf{r}}}, \text{ where } \mathcal{A} \mathcal{A}^* \mathbf{c} = \mathbf{y}.$$

- Discrete-discrete formulation

Assume parametric model for object:

$$f(\vec{\mathbf{r}}) = \sum_{j=1}^N f_j p_j(\vec{\mathbf{r}}).$$

Estimate parameter vector $\mathbf{f} = (f_1, \dots, f_N)$ from data vector \mathbf{y} .

Why Iterative Image Reconstruction?

- “Non-Fourier” physical effects such as field inhomogeneity
- Incorporate prior information, *e.g.*:
 - support constraints
 - (piecewise) smoothness
 - phase constraints
- No density compensation needed
- Statistical modeling may reduce noise

Primary drawbacks of Iterative Methods

- Algorithm speed
- Complexity, *e.g.*, choosing regularization parameter(s)

Model-Based Image Reconstruction: Overview

Model-Based Image Reconstruction

MR signal equation with more complete physics:

$$s(t) = \int f(\vec{r}) s^{\text{coil}}(\vec{r}) e^{-i\omega(\vec{r})t} e^{-R_2^*(\vec{r})t} e^{-i2\pi\vec{k}(t)\cdot\vec{r}} d\vec{r}$$

$$y_i = s(t_i) + \text{noise}_i, \quad i = 1, \dots, M$$

- $s^{\text{coil}}(\vec{r})$ Receive-coil sensitivity pattern(s) (for SENSE)
- $\omega(\vec{r})$ Off-resonance frequency map
(due to field inhomogeneity / magnetic susceptibility)
- $R_2^*(\vec{r})$ Relaxation map

Other physical factors (?)

- Eddy current effects; in $\vec{k}(t)$
- Concomitant gradient terms
- Chemical shift
- Motion

Goal?

(it depends)

Field Inhomogeneity-Corrected Reconstruction

$$s(t) = \int f(\vec{r}) s^{\text{coil}}(\vec{r}) e^{-i\omega(\vec{r})t} e^{-R_2^*(\vec{r})t} e^{-i2\pi\vec{k}(t)\cdot\vec{r}} d\vec{r}$$

Goal: reconstruct $f(\vec{r})$ given field map $\omega(\vec{r})$.
(Assume all other terms are known or unimportant.)

Motivation

Essential for functional MRI of brain regions near sinus cavities!

(Sutton *et al.*, ISMRM 2001; T-MI 2003)

Sensitivity-Encoded (SENSE) Reconstruction

$$s(t) = \int f(\vec{r}) s^{\text{coil}}(\vec{r}) e^{-i\omega(\vec{r})t} e^{-R_2^*(\vec{r})t} e^{-i2\pi\vec{k}(t)\cdot\vec{r}} d\vec{r}$$

Goal: reconstruct $f(\vec{r})$ given sensitivity maps $s^{\text{coil}}(\vec{r})$.
(Assume all other terms are known or unimportant.)

Can combine SENSE with field inhomogeneity correction “easily.”

(Sutton *et al.*, ISMRM 2001, Olafsson *et al.*, ISBI 2006)

Joint Estimation of Image and Field-Map

$$s(t) = \int f(\vec{r}) s^{\text{coil}}(\vec{r}) e^{-i\omega(\vec{r})t} e^{-R_2^*(\vec{r})t} e^{-i2\pi\vec{k}(t)\cdot\vec{r}} d\vec{r}$$

Goal: estimate *both* the image $f(\vec{r})$ and the field map $\omega(\vec{r})$
(Assume all other terms are known or unimportant.)

Analogy:

joint estimation of emission image and attenuation map in PET.

(Sutton *et al.*, ISMRM Workshop, 2001; ISBI 2002; ISMRM 2002;
ISMRM 2003; MRM 2004)

The Kitchen Sink

$$s(t) = \int f(\vec{r}) s^{\text{coil}}(\vec{r}) e^{-i\omega(\vec{r})t} e^{-R_2^*(\vec{r})t} e^{-i2\pi\vec{k}(t)\cdot\vec{r}} d\vec{r}$$

Goal: estimate image $f(\vec{r})$, field map $\omega(\vec{r})$, and relaxation map $R_2^*(\vec{r})$

Requires “suitable” k-space trajectory.

(Sutton *et al.*, ISMRM 2002; Twieg, MRM, 2003)

Estimation of Dynamic Rate Maps

$$s(t) = \int f(\vec{r}) s^{\text{coil}}(\vec{r}) e^{-i\omega(\vec{r})t} e^{-R_2^*(\vec{r})t} e^{-i2\pi\vec{k}(t)\cdot\vec{r}} d\vec{r}$$

Goal: estimate **dynamic** field map $\omega(\vec{r})$ and “BOLD effect” $R_2^*(\vec{r})$ given baseline image $f(\vec{r})$ in fMRI.

Motion...

(Olafsson *et al.*, IEEE T-MI 2008)

Model-Based Image Reconstruction: Details

Basic Signal Model

$$y_i = s(t_i) + \varepsilon_i, \quad E[y_i] = s(t_i) = \int f(\vec{r}) e^{-i2\pi \vec{k}_i \cdot \vec{r}} d\vec{r}$$

Goal: reconstruct $f(\vec{r})$ from $\mathbf{y} = (y_1, \dots, y_M)$.

Series expansion of unknown **object**:

$$f(\vec{r}) \approx \sum_{j=1}^N f_j p(\vec{r} - \vec{r}_j) \leftarrow \text{usually 2D rect functions.}$$

Substituting into **signal model** yields

$$\begin{aligned} E[y_i] &= \int \left[\sum_{j=1}^N f_j p(\vec{r} - \vec{r}_j) \right] e^{-i2\pi \vec{k}_i \cdot \vec{r}} d\vec{r} = \sum_{j=1}^N \left[\int p(\vec{r} - \vec{r}_j) e^{-i2\pi \vec{k}_i \cdot \vec{r}} d\vec{r} \right] f_j \\ &= \sum_{j=1}^N a_{ij} f_j, \quad a_{ij} = P(\vec{k}_i) e^{-i2\pi \vec{k}_i \cdot \vec{r}_j}, \quad p(\vec{r}) \xleftrightarrow{\text{FT}} P(\vec{k}). \end{aligned}$$

Discrete-discrete measurement model with system matrix $\mathbf{A} = \{a_{ij}\}$:

$$\mathbf{y} = \mathbf{A} \mathbf{f} + \boldsymbol{\varepsilon}.$$

Goal: estimate coefficients (pixel values) $\mathbf{f} = (f_1, \dots, f_N)$ from \mathbf{y} .

Least-Squares Estimation

Estimate object by minimizing a simple cost function:

$$\hat{\mathbf{f}} = \arg \min_{\mathbf{f} \in \mathbb{C}^N} \Psi(\mathbf{f}), \quad \Psi(\mathbf{f}) = \|\mathbf{y} - \mathbf{A}\mathbf{f}\|^2$$

- **data fit** term $\|\mathbf{y} - \mathbf{A}\mathbf{f}\|^2$
corresponds to negative log-likelihood of Gaussian distribution
- Equivalent to maximum-likelihood (ML) estimation

Issues:

- computing minimizer rapidly
- stopping iteration (?)
- image quality

Iterative Minimization by Conjugate Gradients

Choose initial guess $\mathbf{f}^{(0)}$ (e.g., fast conjugate phase / gridding).
Iteration (unregularized):

$$\begin{aligned}\mathbf{g}^{(n)} &= \nabla \Psi(\mathbf{f}^{(n)}) = \mathbf{A}'(\mathbf{A}\mathbf{f}^{(n)} - \mathbf{y}) && \text{gradient} \\ \mathbf{p}^{(n)} &= \mathbf{P}\mathbf{g}^{(n)} && \text{precondition} \\ \gamma_n &= \begin{cases} 0, & n = 0 \\ \frac{\langle \mathbf{g}^{(n)}, \mathbf{p}^{(n)} \rangle}{\langle \mathbf{g}^{(n-1)}, \mathbf{p}^{(n-1)} \rangle}, & n > 0 \end{cases} \\ \mathbf{d}^{(n)} &= -\mathbf{p}^{(n)} + \gamma_n \mathbf{d}^{(n-1)} && \text{search direction} \\ \mathbf{v}^{(n)} &= \mathbf{A}\mathbf{d}^{(n)} \\ \alpha_n &= \langle \mathbf{d}^{(n)}, -\mathbf{g}^{(n)} \rangle / \|\mathbf{v}^{(n)}\|^2 && \text{step size} \\ \mathbf{f}^{(n+1)} &= \mathbf{f}^{(n)} + \alpha_n \mathbf{d}^{(n)} && \text{update}\end{aligned}$$

Bottlenecks: computing $\mathbf{A}\mathbf{f}^{(n)}$ and $\mathbf{A}'\mathbf{r}$.

- \mathbf{A} is too large to store explicitly (not sparse)
- Even if \mathbf{A} were stored, directly computing $\mathbf{A}\mathbf{f}$ is $O(MN)$ per iteration, whereas FFT is only $O(M \log M)$.

Computing $\mathbf{A}f$ Rapidly

$$[\mathbf{A}f]_i = \sum_{j=1}^N a_{ij} f_j = P(\vec{\mathbf{k}}_i) \sum_{j=1}^N e^{-i2\pi\vec{\mathbf{k}}_i \cdot \vec{r}_j} f_j, \quad i = 1, \dots, M$$

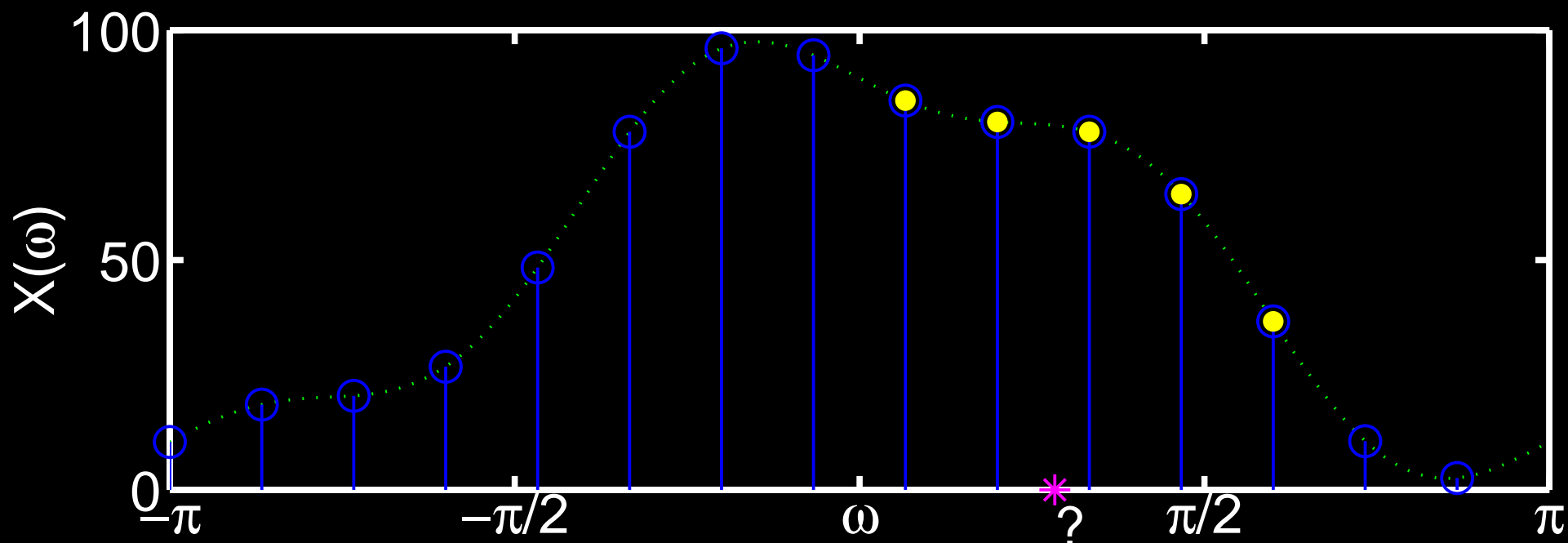
- Pixel locations $\{\vec{r}_j\}$ are uniformly spaced
- k-space locations $\{\vec{\mathbf{k}}_i\}$ are unequally spaced

\implies needs nonuniform fast Fourier transform (NUFFT)

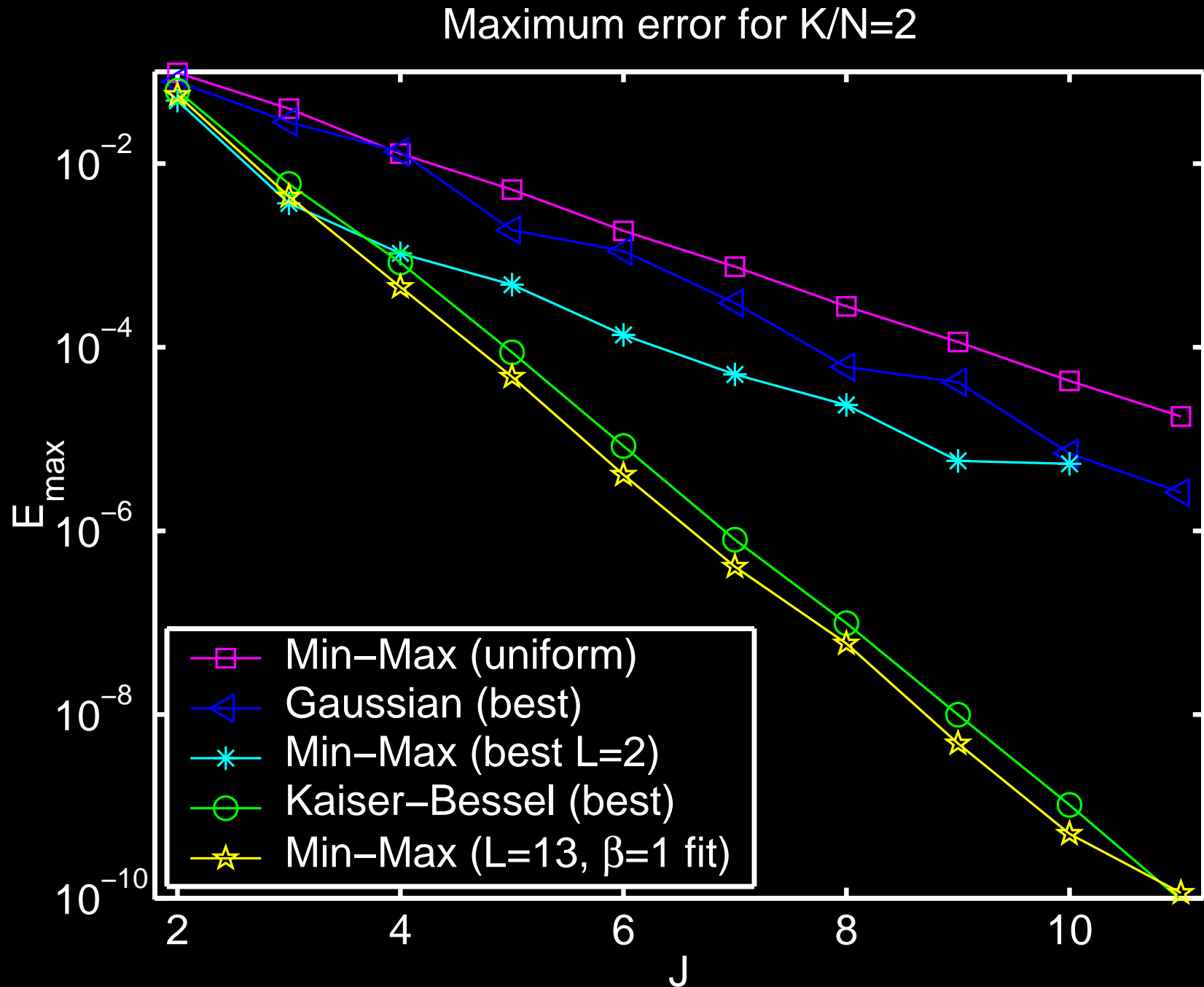
NUFFT (Type 2)

- Compute **over-sampled FFT** of equally-spaced signal samples
- **Interpolate** onto desired unequally-spaced frequency locations
- Dutt & Rokhlin, SIAM JSC, 1993, Gaussian bell interpolator
- Fessler & Sutton, IEEE T-SP, 2003, min-max interpolator and min-max optimized Kaiser-Bessel interpolator.

NUFFT toolbox: <http://www.eecs.umich.edu/~fessler/code>



Worst-Case NUFFT Interpolation Error



NUFFT Interpolation

Ideal interpolator would be (impractical) sinc-like (Dirichlet kernel)

In practice, we use finite-support frequency-domain interpolators; these have nonuniform spatial response.

Spatial “scaling” of the signal before FFT is necessary to compensate for imperfect interpolation.

Open problem: determining optimal scaling function.
(Reciprocal of Fourier transform of Kaiser-Bessel function works reasonably well.)

Further Acceleration using Toeplitz Matrices

Cost-function gradient:

$$\begin{aligned}\mathbf{g}^{(n)} &= \mathbf{A}'(\mathbf{A}\mathbf{f}^{(n)} - \mathbf{y}) \\ &= \mathbf{T}\mathbf{f}^{(n)} - \mathbf{b},\end{aligned}$$

where

$$\mathbf{T} \triangleq \mathbf{A}'\mathbf{A}, \quad \mathbf{b} \triangleq \mathbf{A}'\mathbf{y}.$$

In the absence of field inhomogeneity, the Gram matrix \mathbf{T} is **Toeplitz**:

$$[\mathbf{A}'\mathbf{A}]_{jk} = \sum_{i=1}^M |P(\vec{\mathbf{k}}_i)|^2 e^{-i2\pi \vec{\mathbf{k}}_i \cdot (\vec{r}_j - \vec{r}_k)}.$$

Computing $\mathbf{T}\mathbf{f}^{(n)}$ requires an ordinary ($2\times$ over-sampled) FFT.

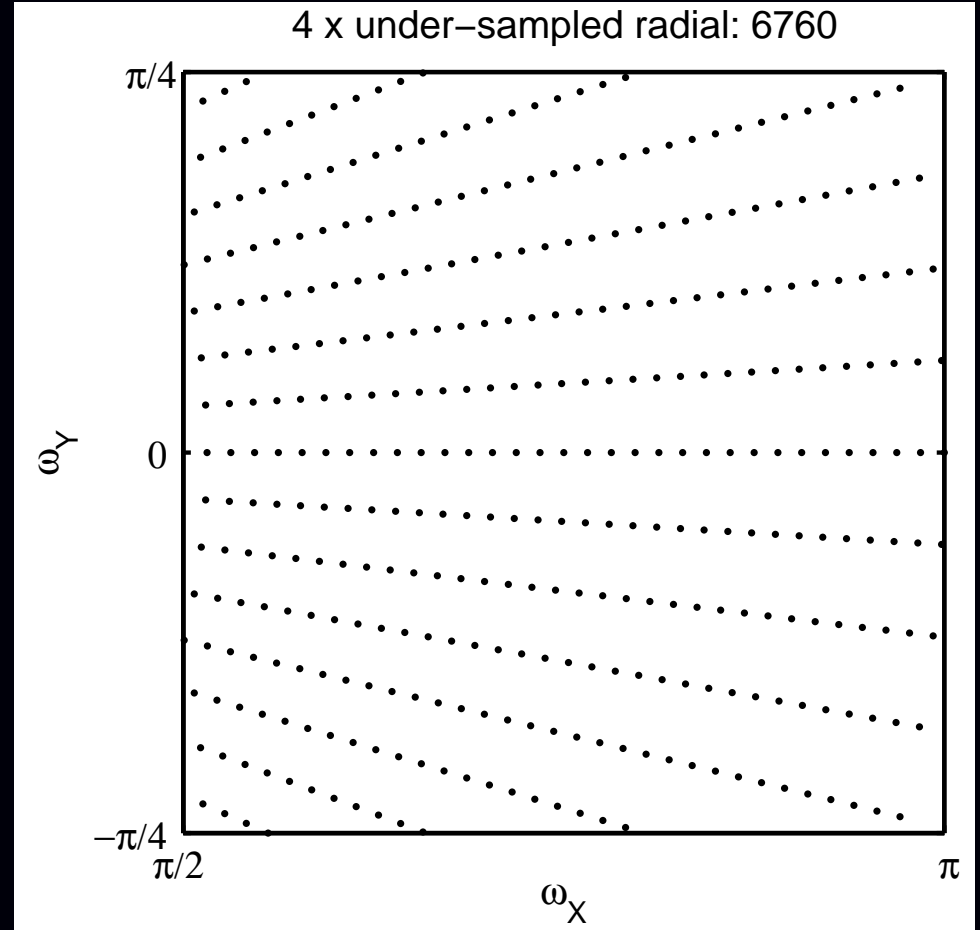
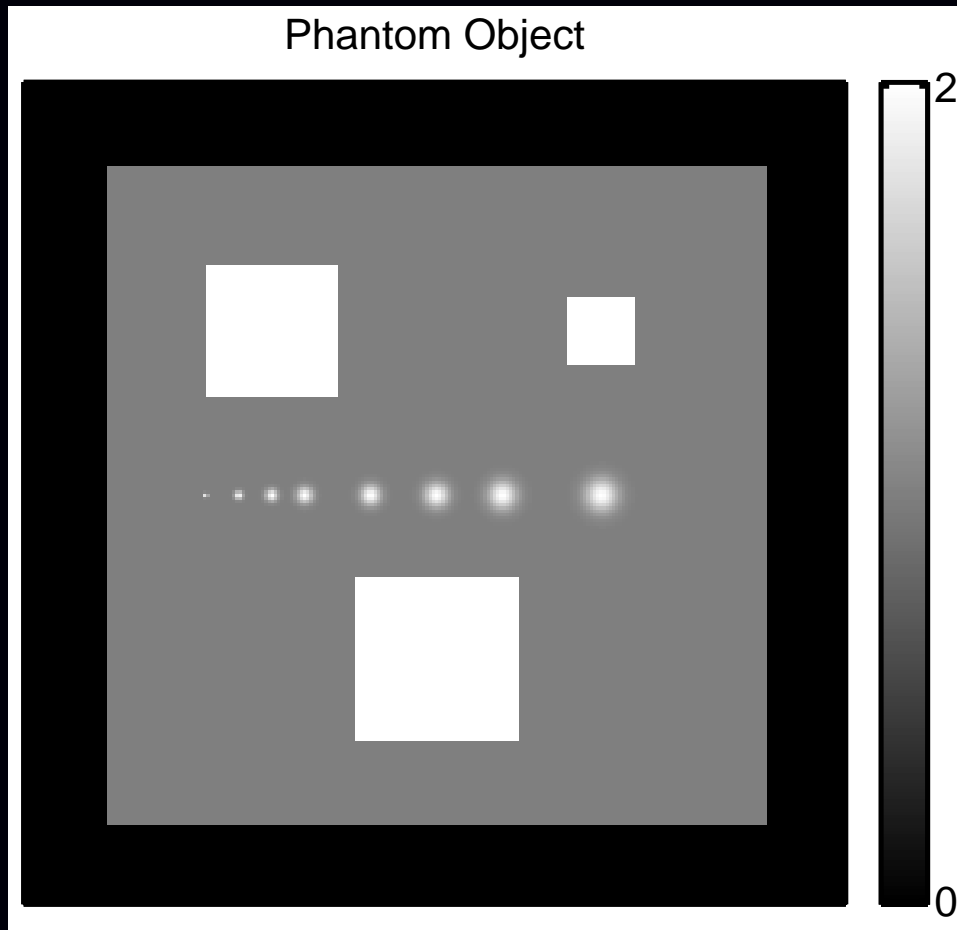
(Chan & Ng, SIAM Review, 1996)

In 2D: block Toeplitz with Toeplitz blocks (BTTB).

Precomputing the first column of \mathbf{T} and \mathbf{b} requires a couple NUFFTs.
(Wajer, ISMRM 2001, Eggers ISMRM 2002, Liu ISMRM 2005)

This formulation seems ideal for “hardware” FFT systems.

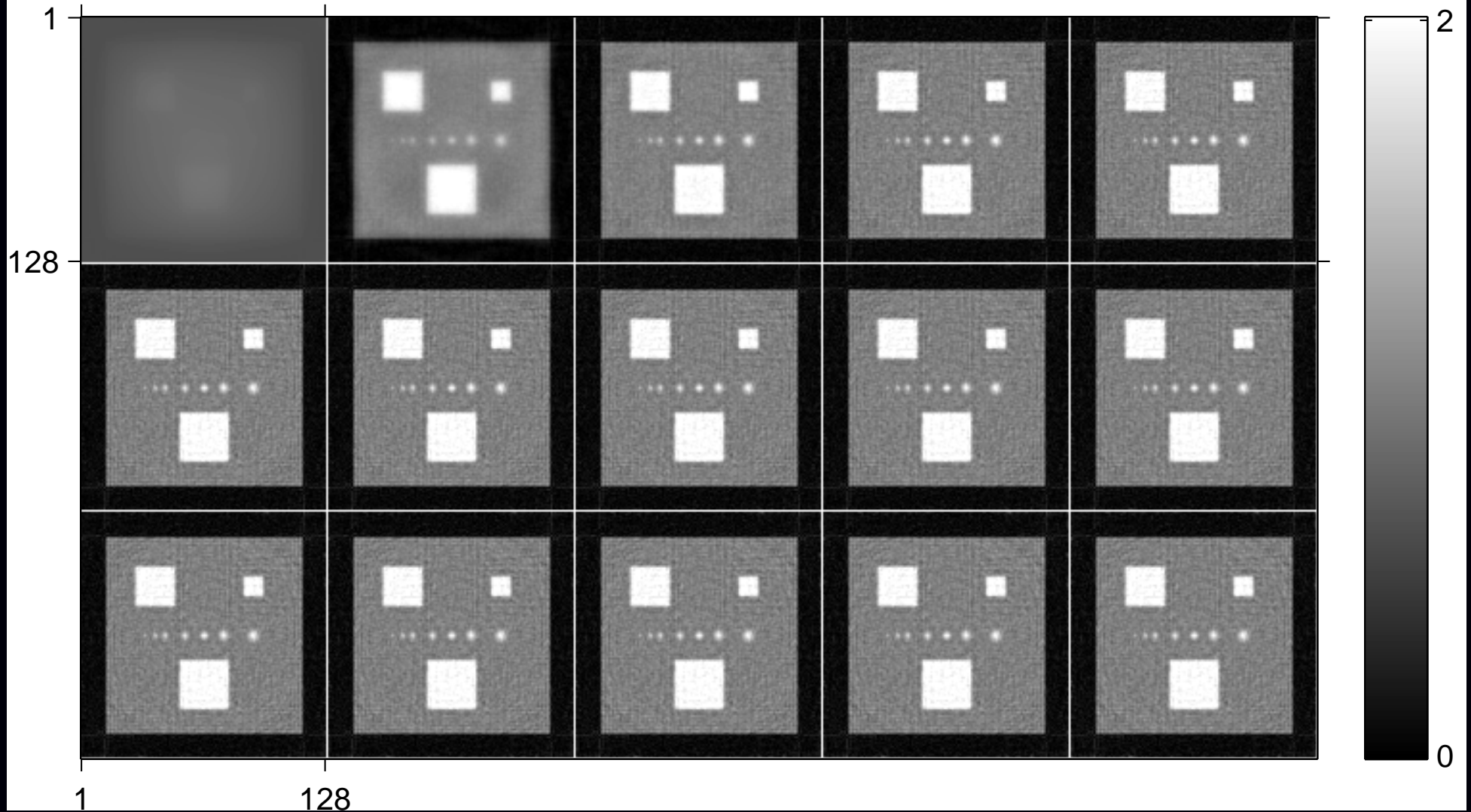
Unregularized Example: Simulated Data



4x under-sampled radial k-space data
Analytical k-space data generation

Unregularized Example: Images

Unregularized CG, 1:4:60, SNR=40

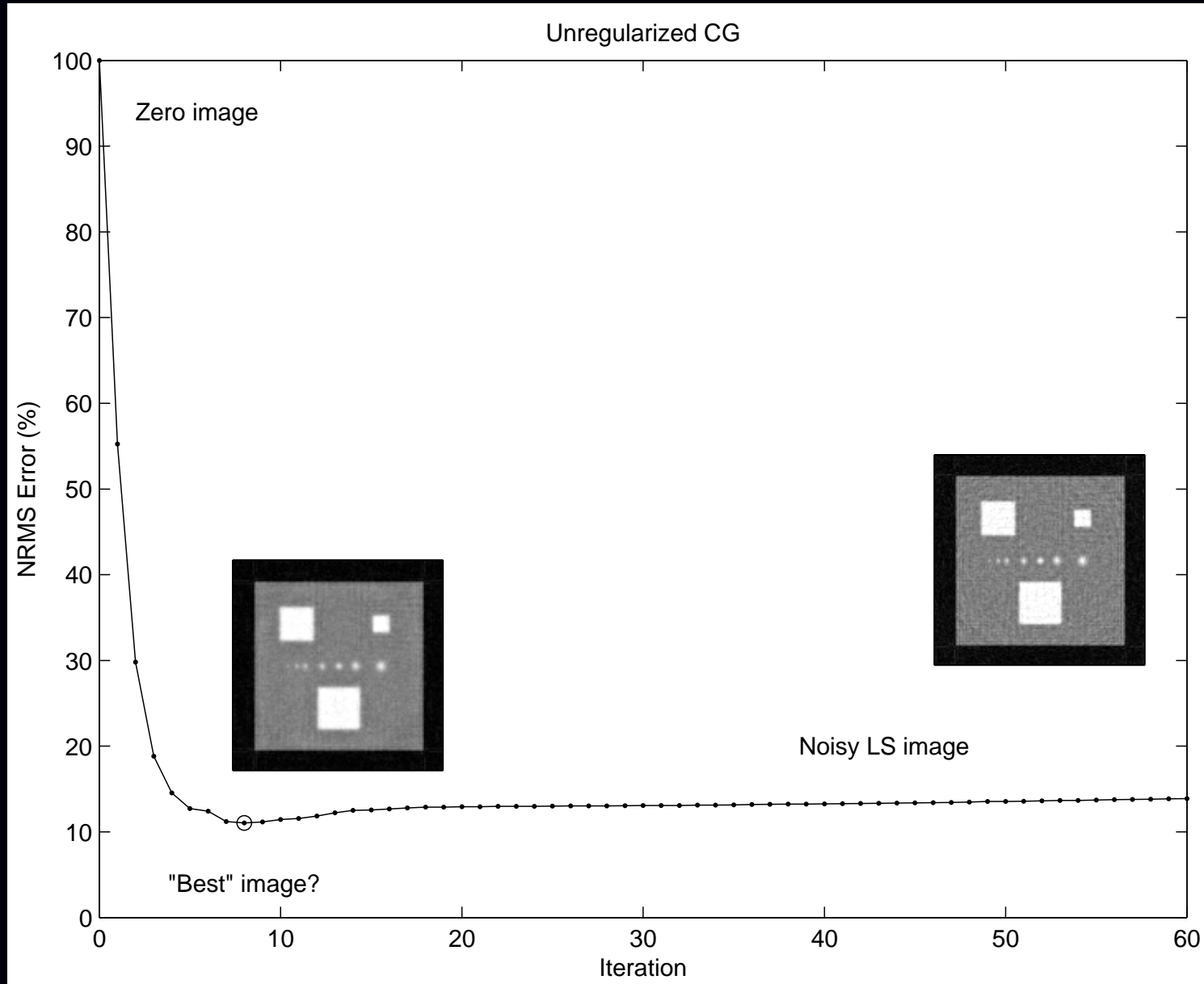


Iterations 1:4:60 of unregularized CG reconstruction

Unregularized Example: Movie

(movie in pdf)

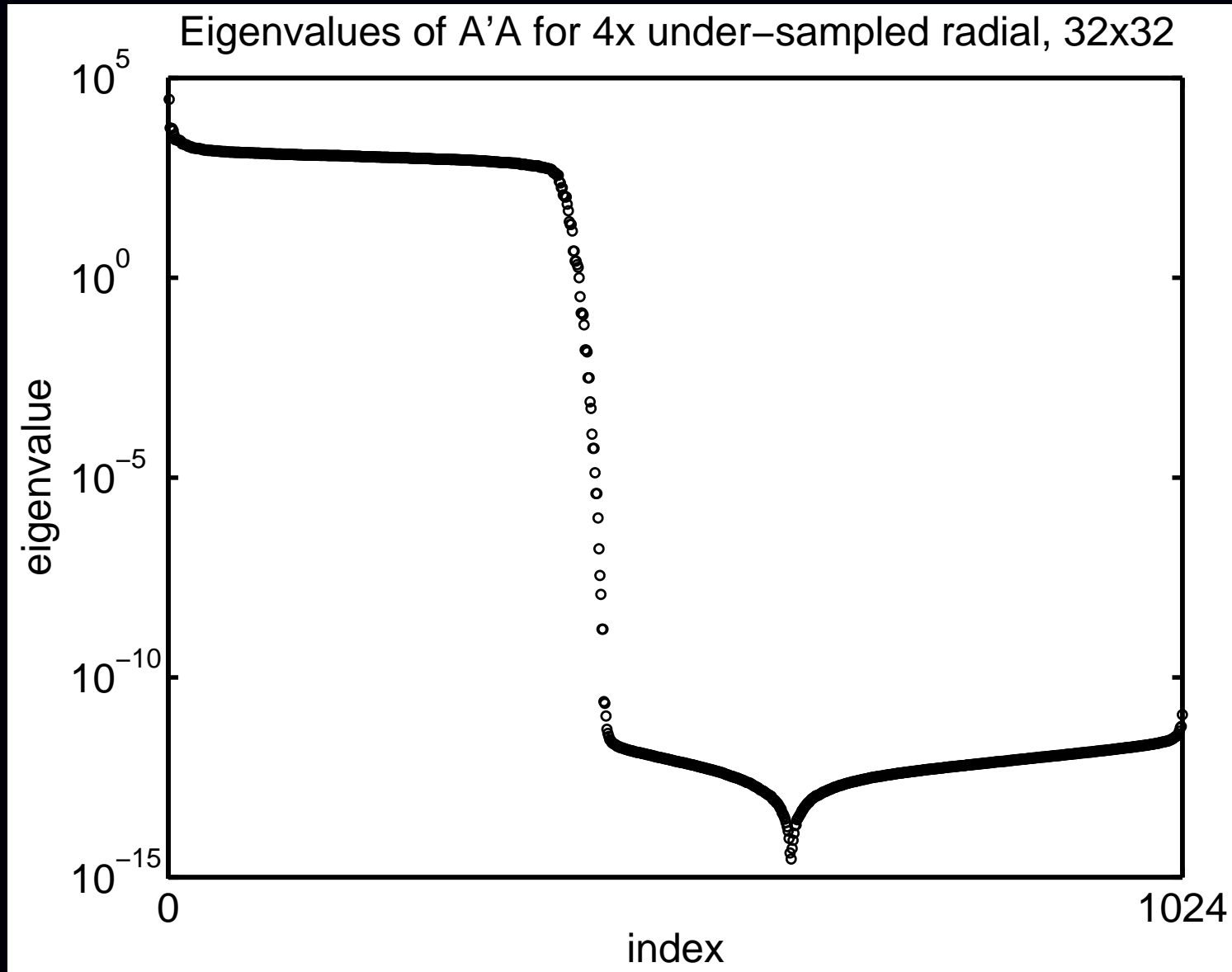
Unregularized Example: RMS Error



Complexity: when to stop?

A solution: regularization.

Unregularized Eigenspectrum

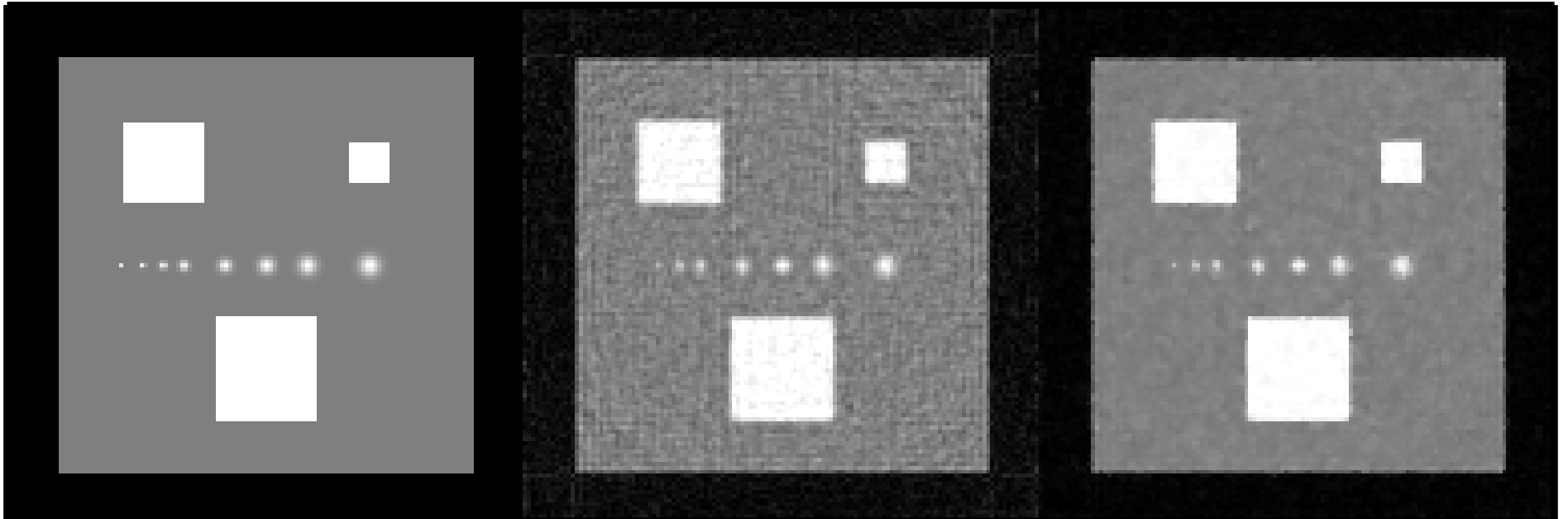


Regularized Example: Movie

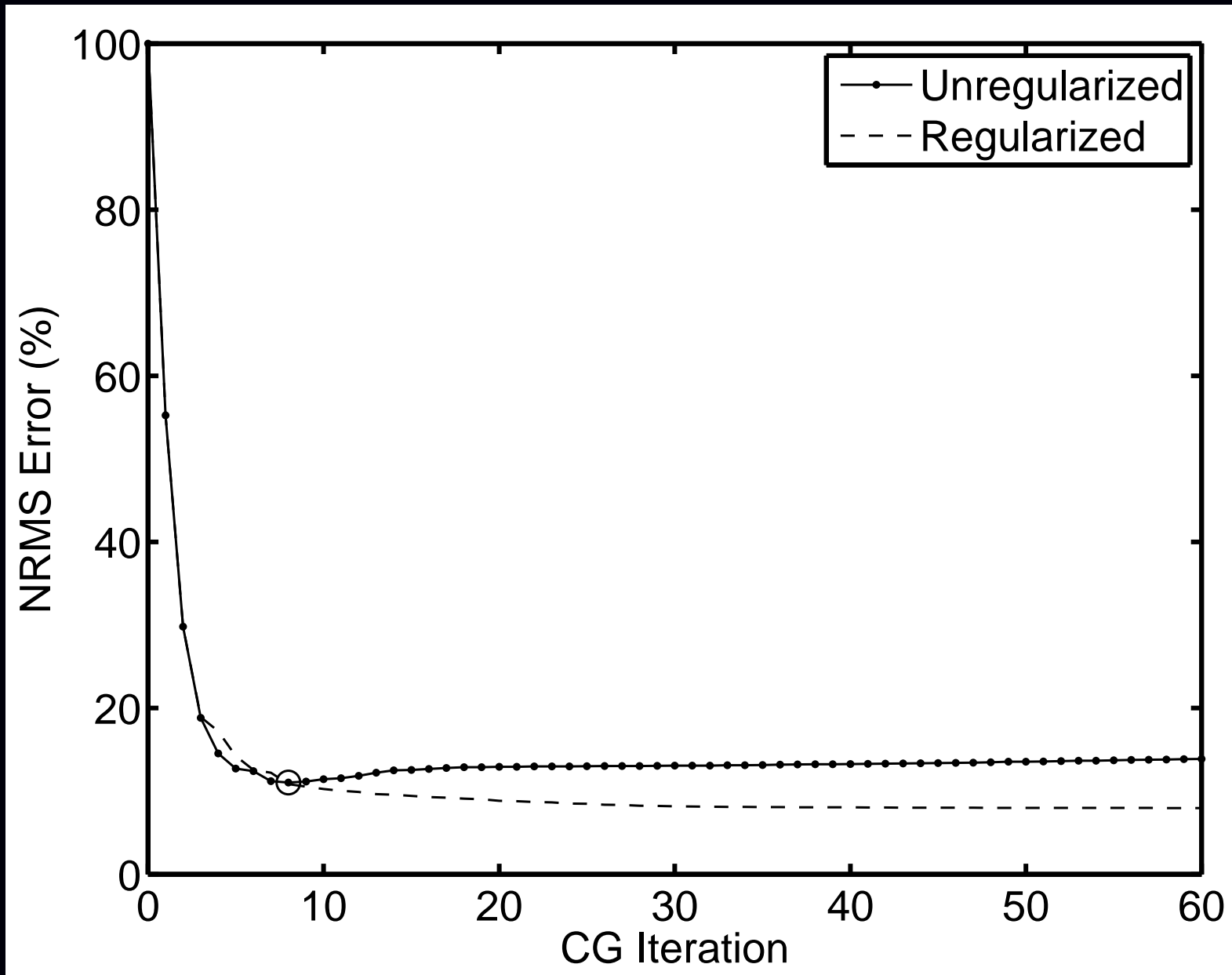
(movie in pdf)

Regularized Example: Image Comparison

True | Unregularized | Edge preserving regularization



Regularized Example: RMS Error



Regularized Least-Squares Estimation

Estimate object by minimizing a *regularized* cost function:

$$\hat{\mathbf{f}} = \arg \min_{\mathbf{f} \in \mathbb{C}^N} \Psi(\mathbf{f}), \quad \Psi(\mathbf{f}) = \|\mathbf{y} - \mathbf{A}\mathbf{f}\|^2 + \alpha R(\mathbf{f})$$

- **data fit** term $\|\mathbf{y} - \mathbf{A}\mathbf{f}\|^2$
corresponds to negative log-likelihood of Gaussian distribution
- **regularizing** term $R(\mathbf{f})$ controls noise by penalizing roughness,

$$\text{e.g. : } R(\mathbf{f}) \approx \int \|\nabla f\|^2 d\vec{r}$$

- **regularization parameter** $\alpha > 0$
controls tradeoff between spatial resolution and noise
- Equivalent to Bayesian MAP estimation with prior $\propto e^{-\alpha R(\mathbf{f})}$

Complexities:

- choosing $R(\mathbf{f})$
- choosing α
- computing minimizer rapidly.

Quadratic regularization

1D example: squared differences between neighboring pixel values:

$$R(f) = \sum_{j=2}^N \frac{1}{2} |f_j - f_{j-1}|^2.$$

In matrix-vector notation, $R(f) = \frac{1}{2} \|\mathbf{C}f\|^2$ where

$$\mathbf{C} = \begin{bmatrix} -1 & 1 & 0 & 0 & \dots & 0 \\ 0 & -1 & 1 & 0 & \dots & 0 \\ & & & \ddots & \ddots & \\ 0 & \dots & 0 & 0 & -1 & 1 \end{bmatrix}, \text{ so } \mathbf{C}f = \begin{bmatrix} f_2 - f_1 \\ \vdots \\ f_N - f_{N-1} \end{bmatrix}.$$

For 2D and higher-order differences, modify differencing matrix \mathbf{C} .

Leads to closed-form solution:

$$\begin{aligned} \hat{f} &= \arg \min_f \|\mathbf{y} - \mathbf{A}f\|^2 + \alpha \|\mathbf{C}f\|^2 \\ &= [\mathbf{A}'\mathbf{A} + \alpha \mathbf{C}'\mathbf{C}]^{-1} \mathbf{A}'\mathbf{y}. \end{aligned}$$

(a formula of limited practical use for computing \hat{f})

Choosing the Regularization Parameter

Spatial resolution analysis (Fessler & Rogers, IEEE T-IP, 1996):

$$\hat{\mathbf{f}} = [\mathbf{A}'\mathbf{A} + \alpha\mathbf{C}'\mathbf{C}]^{-1} \mathbf{A}'\mathbf{y}$$
$$E[\hat{\mathbf{f}}] = [\mathbf{A}'\mathbf{A} + \alpha\mathbf{C}'\mathbf{C}]^{-1} \mathbf{A}'E[\mathbf{y}]$$
$$E[\hat{\mathbf{f}}] = \underbrace{[\mathbf{A}'\mathbf{A} + \alpha\mathbf{C}'\mathbf{C}]^{-1} \mathbf{A}'\mathbf{A}}_{\text{blur}} \mathbf{f}$$

$\mathbf{A}'\mathbf{A}$ and $\mathbf{C}'\mathbf{C}$ are Toeplitz \implies blur is approximately shift-invariant.

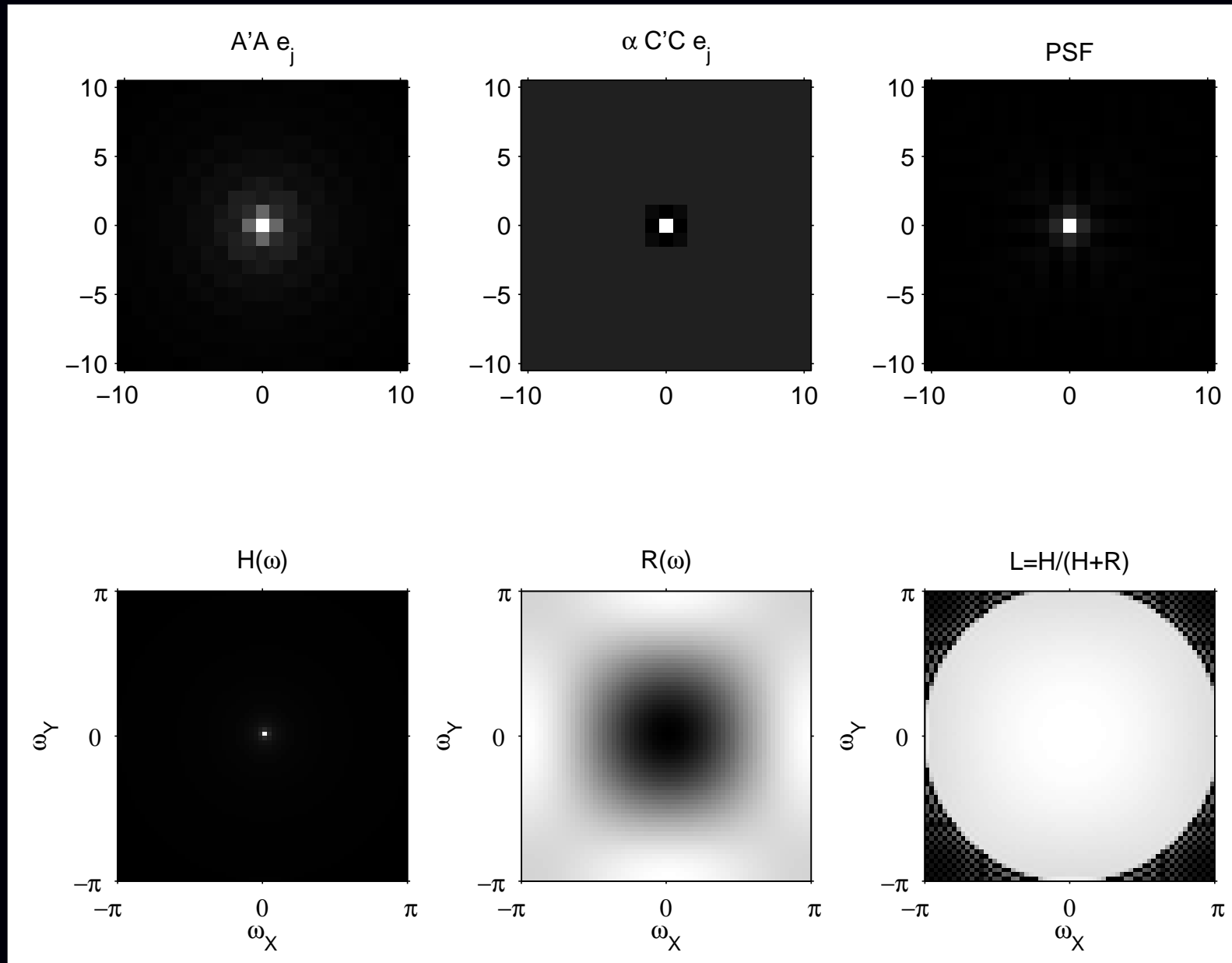
Frequency response of blur:

$$L(\omega) = \frac{H(\omega)}{H(\omega) + \alpha R(\omega)}$$

- $H(\omega_k) = \text{FFT}(\mathbf{A}'\mathbf{A} e_j)$ (lowpass)
- $R(\omega_k) = \text{FFT}(\mathbf{C}'\mathbf{C} e_j)$ (highpass)

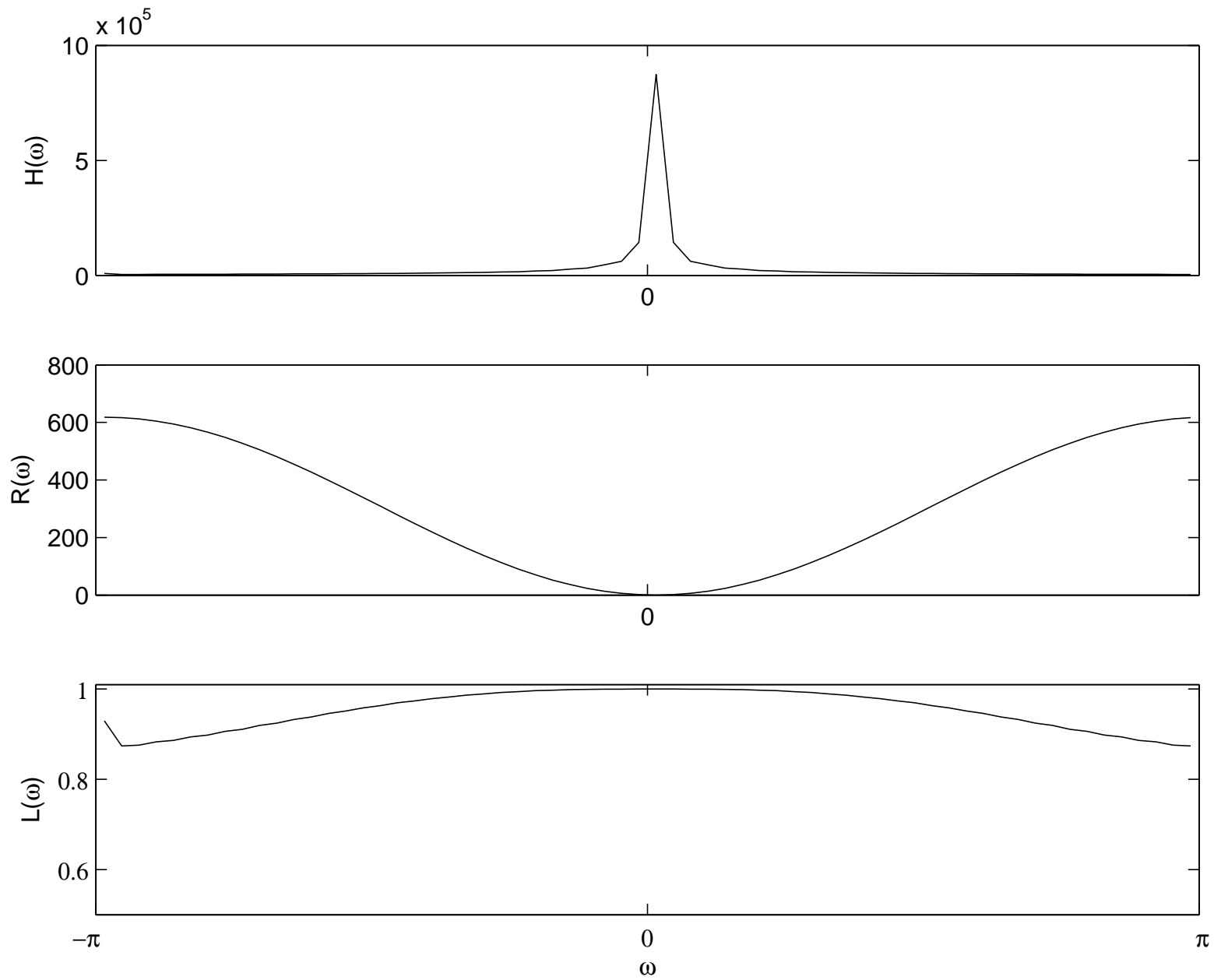
Adjust α to achieve desired spatial resolution.

Spatial Resolution Example

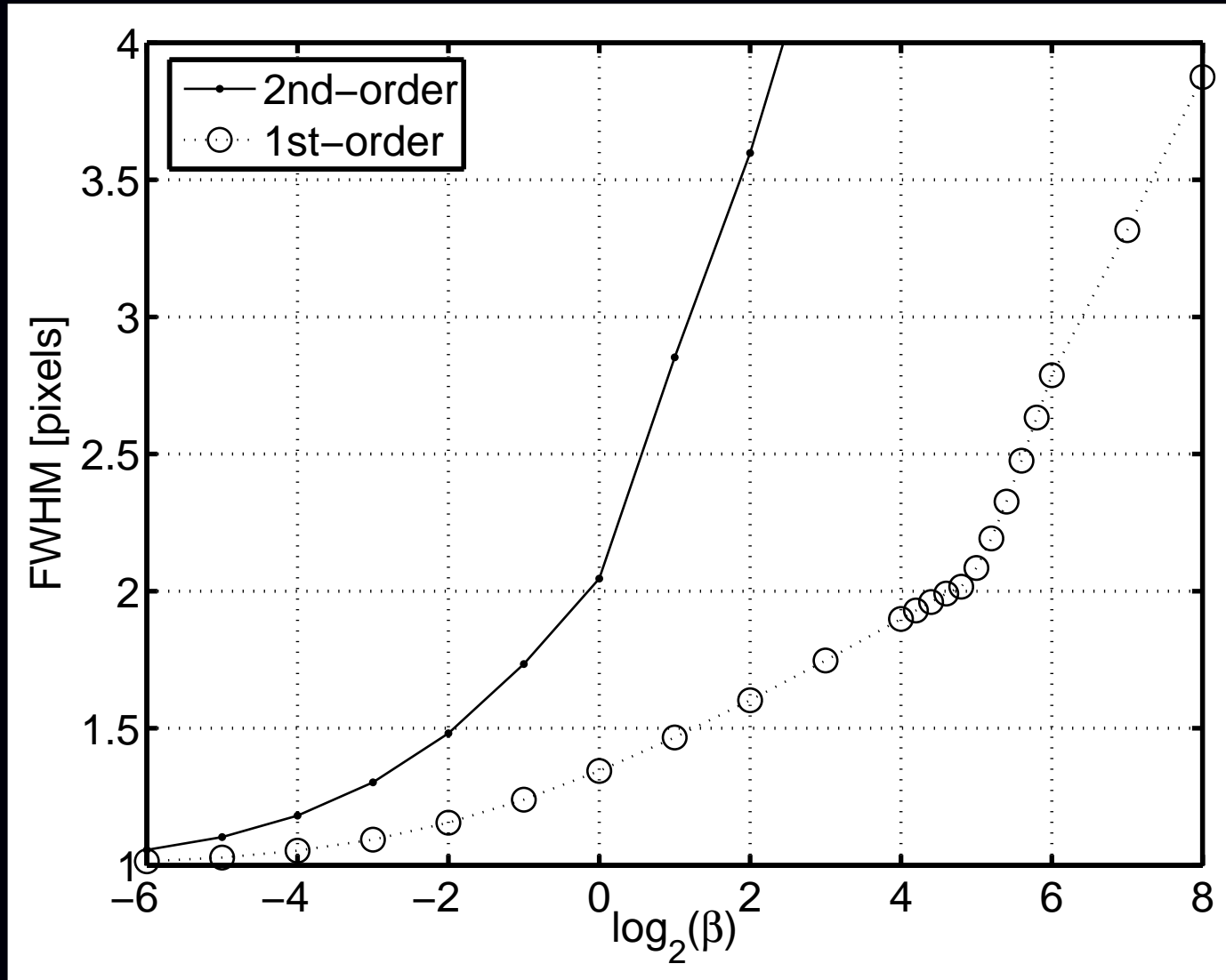


Radial k-space trajectory, FWHM of PSF is 1.2 pixels

Spatial Resolution Example: Profiles



Tabulating Spatial Resolution vs Regularization



Trajectory specific, but easily computed using a few FFTs
Works only for quadratic regularization

Resolution/noise tradeoffs

Noise analysis:

$$\text{Cov}\{\hat{\mathbf{f}}\} = [\mathbf{A}'\mathbf{A} + \alpha\mathbf{C}'\mathbf{C}]^{-1} \mathbf{A}' \text{Cov}\{\mathbf{y}\} \mathbf{A} [\mathbf{A}'\mathbf{A} + \alpha\mathbf{C}'\mathbf{C}]^{-1}$$

Using circulant approximations to $\mathbf{A}'\mathbf{A}$ and $\mathbf{C}'\mathbf{C}$ yields:

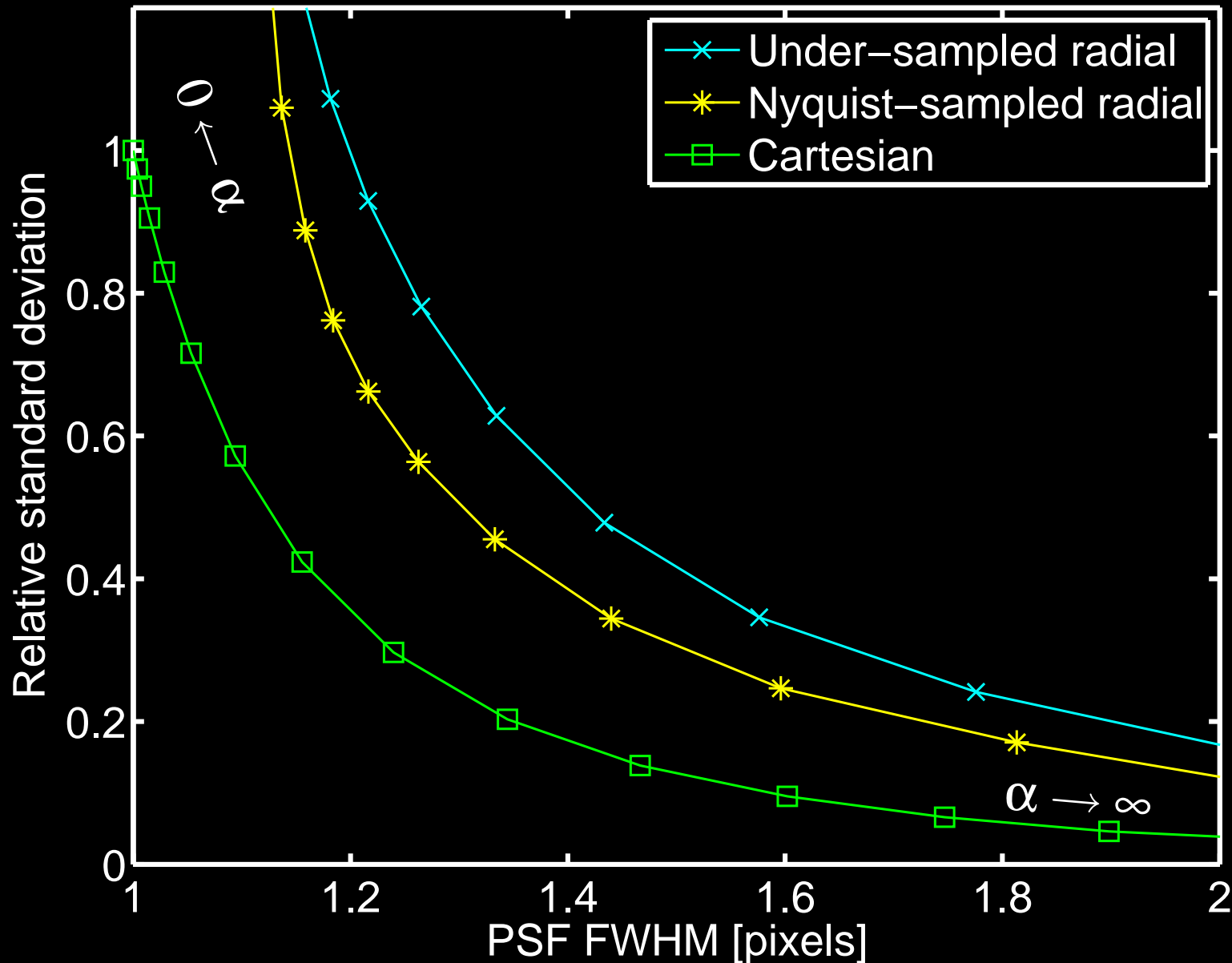
$$\text{Var}\{\hat{f}_j\} \approx \sigma_\varepsilon^2 \sum_k \frac{H(\omega_k)}{(H(\omega_k) + \alpha R(\omega_k))^2}$$

- $H(\omega_k) = \text{FFT}(\mathbf{A}'\mathbf{A} e_j)$ (lowpass)
- $R(\omega_k) = \text{FFT}(\mathbf{C}'\mathbf{C} e_j)$ (highpass)

⇒ Predicting reconstructed image noise requires just 2 FFTs.
(cf. gridding approach?)

Adjust α to achieve desired spatial resolution / noise tradeoff.

Resolution/Noise Tradeoff Example



In short: one can choose α rapidly and predictably for quadratic regularization.

NUFFT with Field Inhomogeneity?

Combine NUFFT with min-max temporal interpolator
(Sutton *et al.*, IEEE T-MI, 2003)
(forward version of “time segmentation”, Noll, T-MI, 1991)

Recall signal model including **field inhomogeneity**:

$$s(t) = \int f(\vec{r}) e^{-i\omega(\vec{r})t} e^{-i2\pi\vec{k}(t)\cdot\vec{r}} d\vec{r}.$$

Temporal interpolation approximation (aka “time segmentation”):

$$e^{-i\omega(\vec{r})t} \approx \sum_{l=1}^L a_l(t) e^{-i\omega(\vec{r})\tau_l}$$

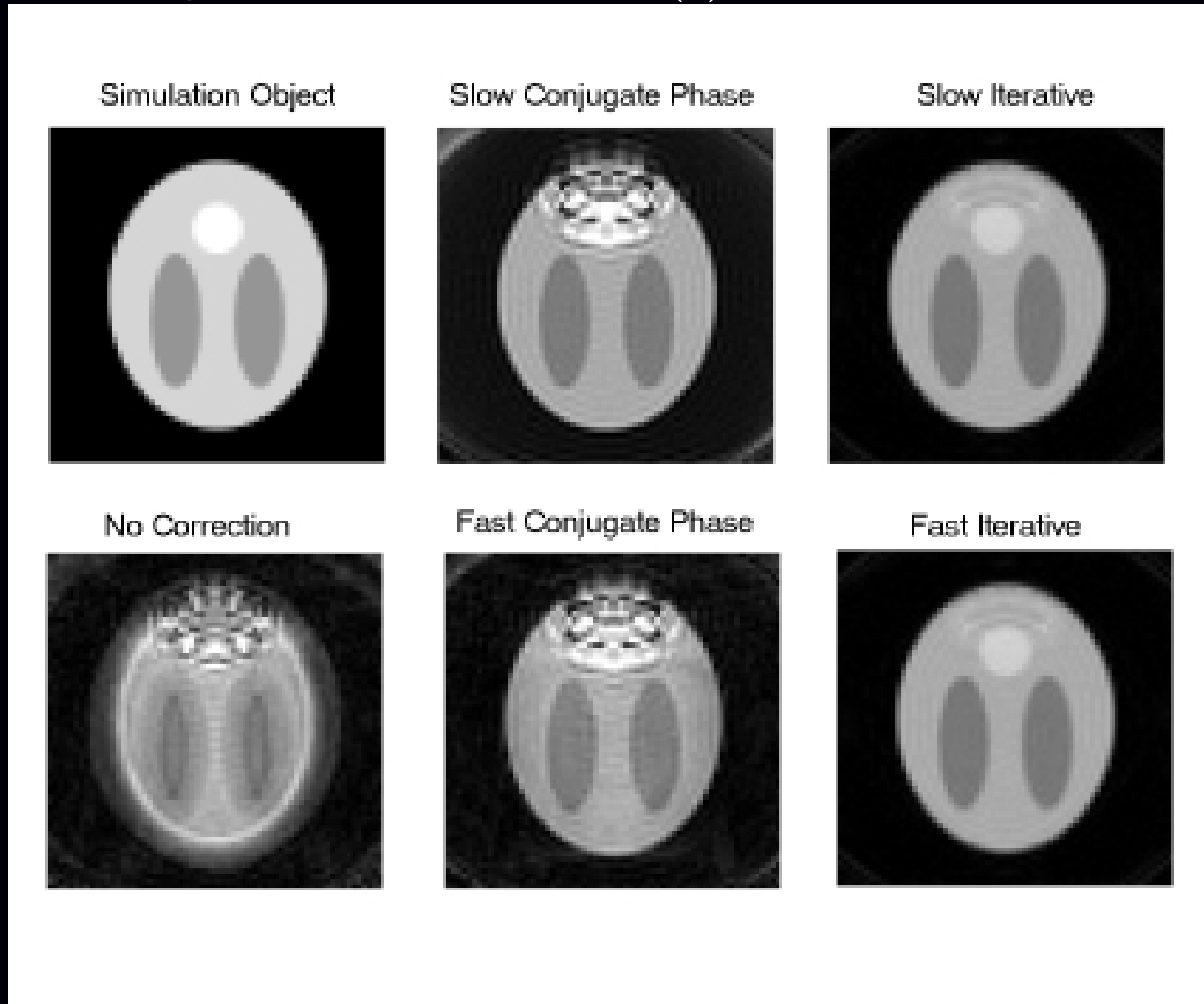
for min-max optimized temporal interpolation functions $\{a_l(\cdot)\}_{l=1}^L$.

$$s(t) \approx \sum_{l=1}^L a_l(t) \int \left[f(\vec{r}) e^{-i\omega(\vec{r})\tau_l} \right] e^{-i2\pi\vec{k}(t)\cdot\vec{r}} d\vec{r}$$

Linear combination of L NUFFT calls.

Field Corrected Reconstruction Example

Simulation using known field map $\omega(\vec{r})$.



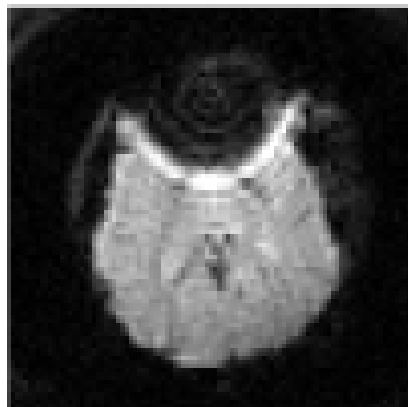
Simulation Quantitative Comparison

- Computation time?
- NRMSE between \hat{f} and f^{true} ?

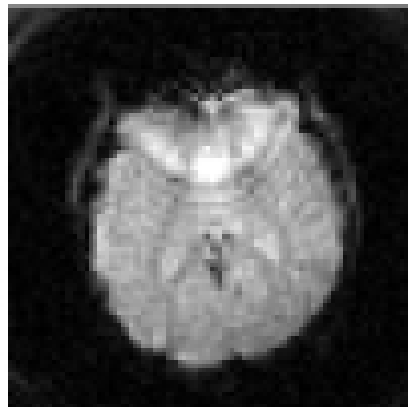
Reconstruction Method	Time (s)	NRMSE	
		complex	magnitude
No Correction	0.06	1.35	0.22
Full Conjugate Phase	4.07	0.31	0.19
Fast Conjugate Phase	0.33	0.32	0.19
Fast Iterative (10 iters)	2.20	0.04	0.04
Exact Iterative (10 iters)	128.16	0.04	0.04

Human Data: Field Correction

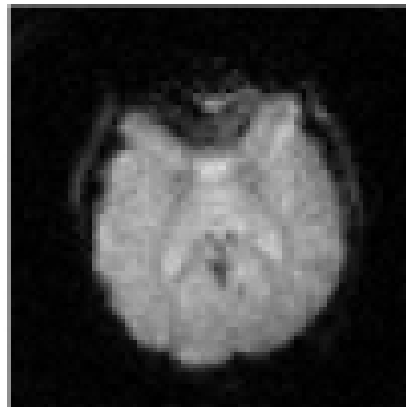
Uncorrected



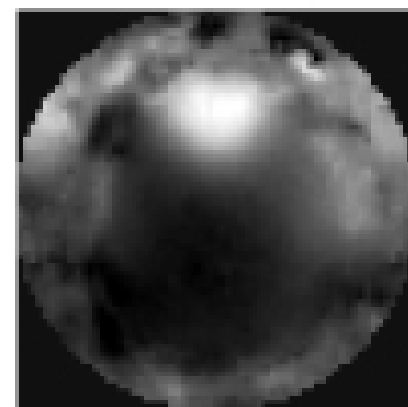
Conjugate Phase



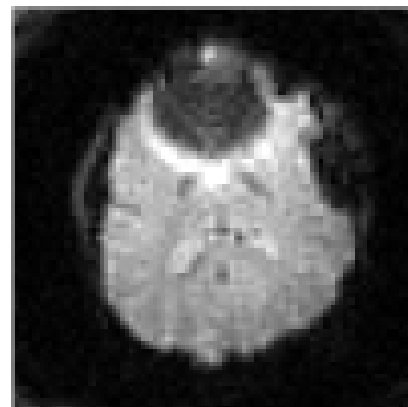
Fast Iterative



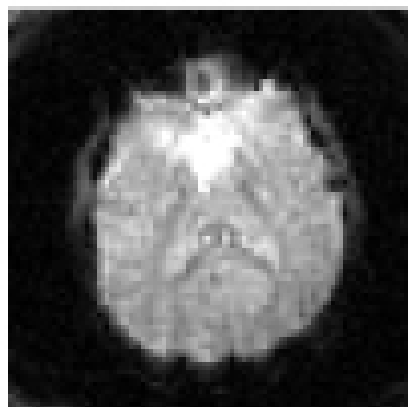
Field Map (Hz)



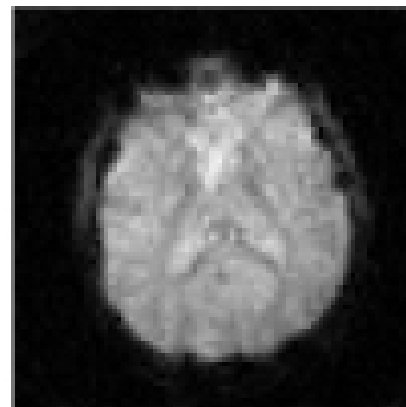
Uncorrected



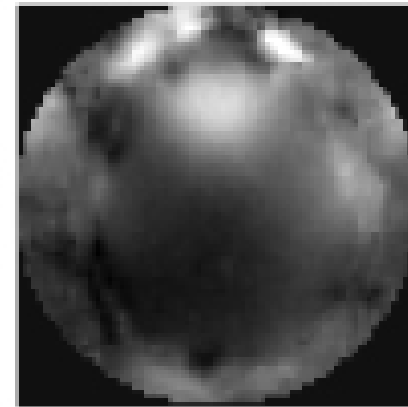
Conjugate Phase



Fast Iterative



Field Map (Hz)



Joint Field-Map / Image Reconstruction

Signal model:

$$y_i = s(t_i) + \varepsilon_i, \quad s(t) = \int f(\vec{r}) e^{-i\omega(\vec{r})t} e^{-i2\pi\vec{k}(t)\cdot\vec{r}} d\vec{r}.$$

After discretization:

$$\mathbf{y} = \mathbf{A}(\boldsymbol{\omega}) \mathbf{f} + \boldsymbol{\varepsilon}, \quad a_{ij}(\boldsymbol{\omega}) = P(\vec{\mathbf{k}}_i) e^{-i\omega_j t_i} e^{-i2\pi\vec{\mathbf{k}}_i \cdot \vec{r}_j}.$$

Joint estimation via regularized (nonlinear) least-squares:

$$(\hat{\mathbf{f}}, \hat{\boldsymbol{\omega}}) = \arg \min_{\mathbf{f} \in \mathbb{C}^N, \boldsymbol{\omega} \in \mathbb{R}^N} \|\mathbf{y} - \mathbf{A}(\boldsymbol{\omega}) \mathbf{f}\|^2 + \beta_1 R_1(\mathbf{f}) + \beta_2 R_2(\boldsymbol{\omega}).$$

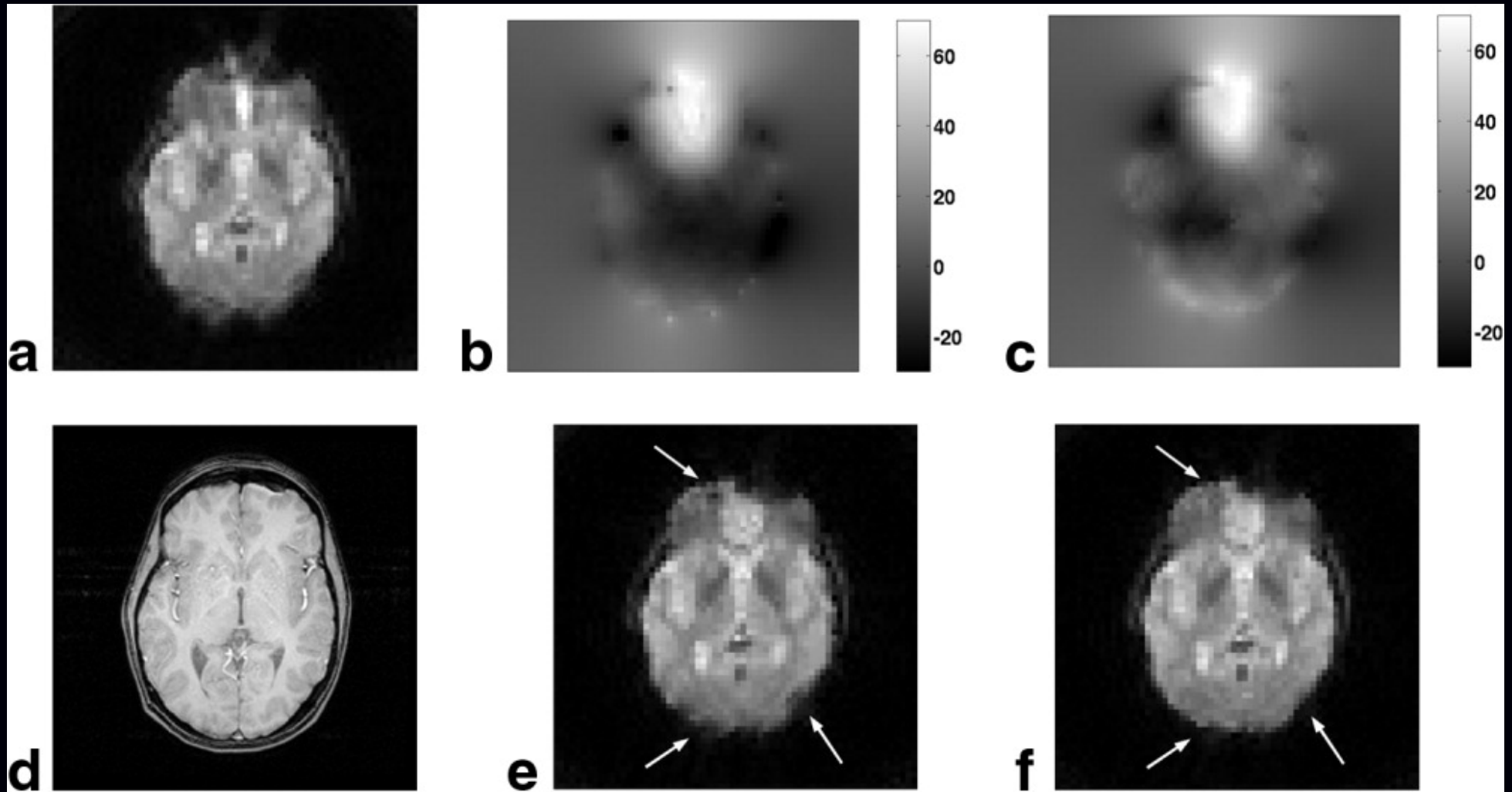
Alternating minimization:

- Using current estimate of fieldmap $\hat{\boldsymbol{\omega}}$, update $\hat{\mathbf{f}}$ using CG algorithm.
- Using current estimate $\hat{\mathbf{f}}$ of image, update fieldmap $\hat{\boldsymbol{\omega}}$ using gradient descent.

Use spiral-in / spiral-out sequence or “racetrack” EPI.

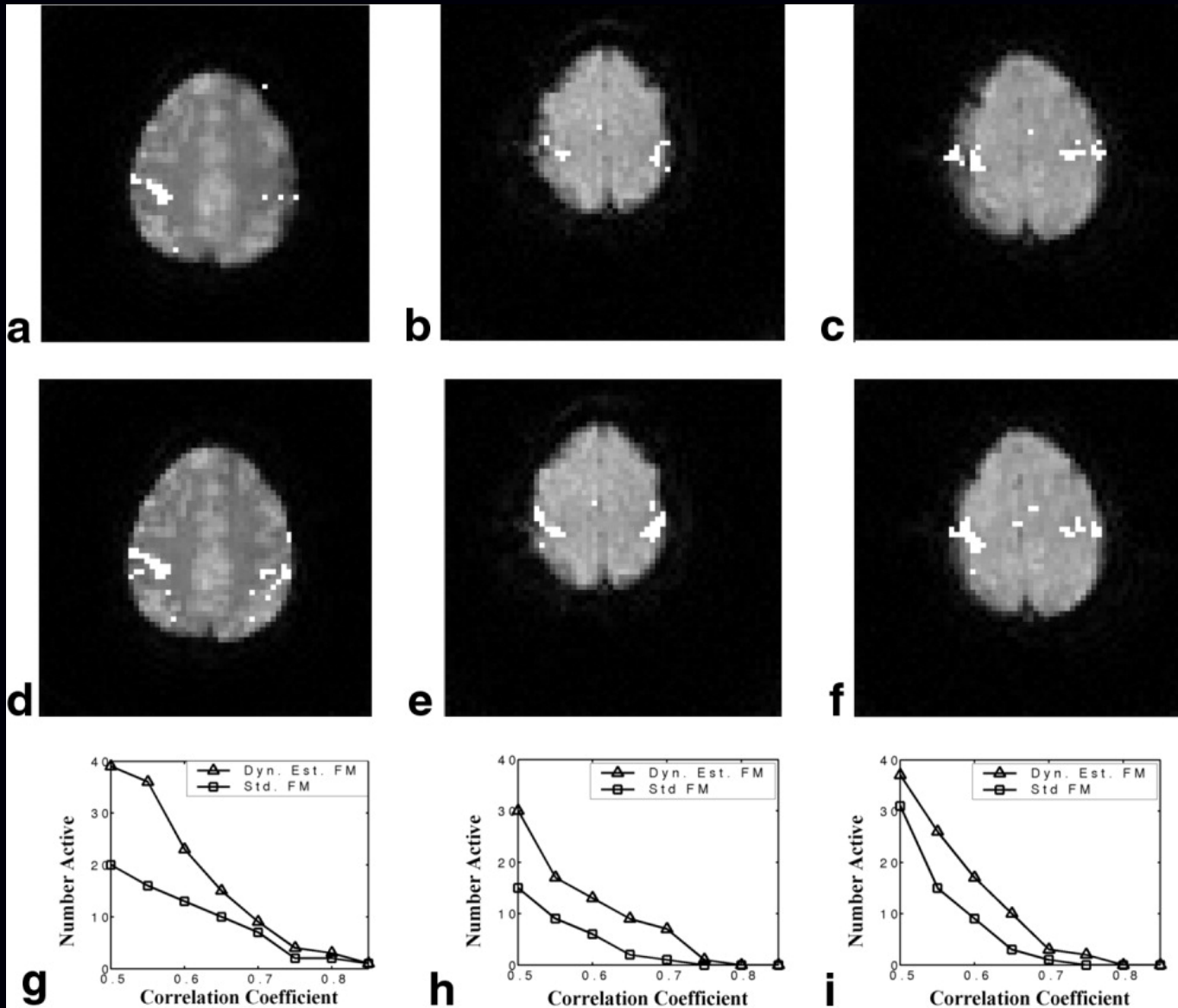
(Sutton *et al.*, MRM, 2004)

Joint Estimation Example



(a) uncorr., (b) std. map, (c) joint map, (d) T1 ref, (e) using std, (f) using joint.

Activation Results: Static vs Dynamic Field Maps



Functional results for the two reconstructions for 3 human subjects.

Reconstruction using the standard field map
for (a) subject 1, (b) subject 2, and (c) subject 3.

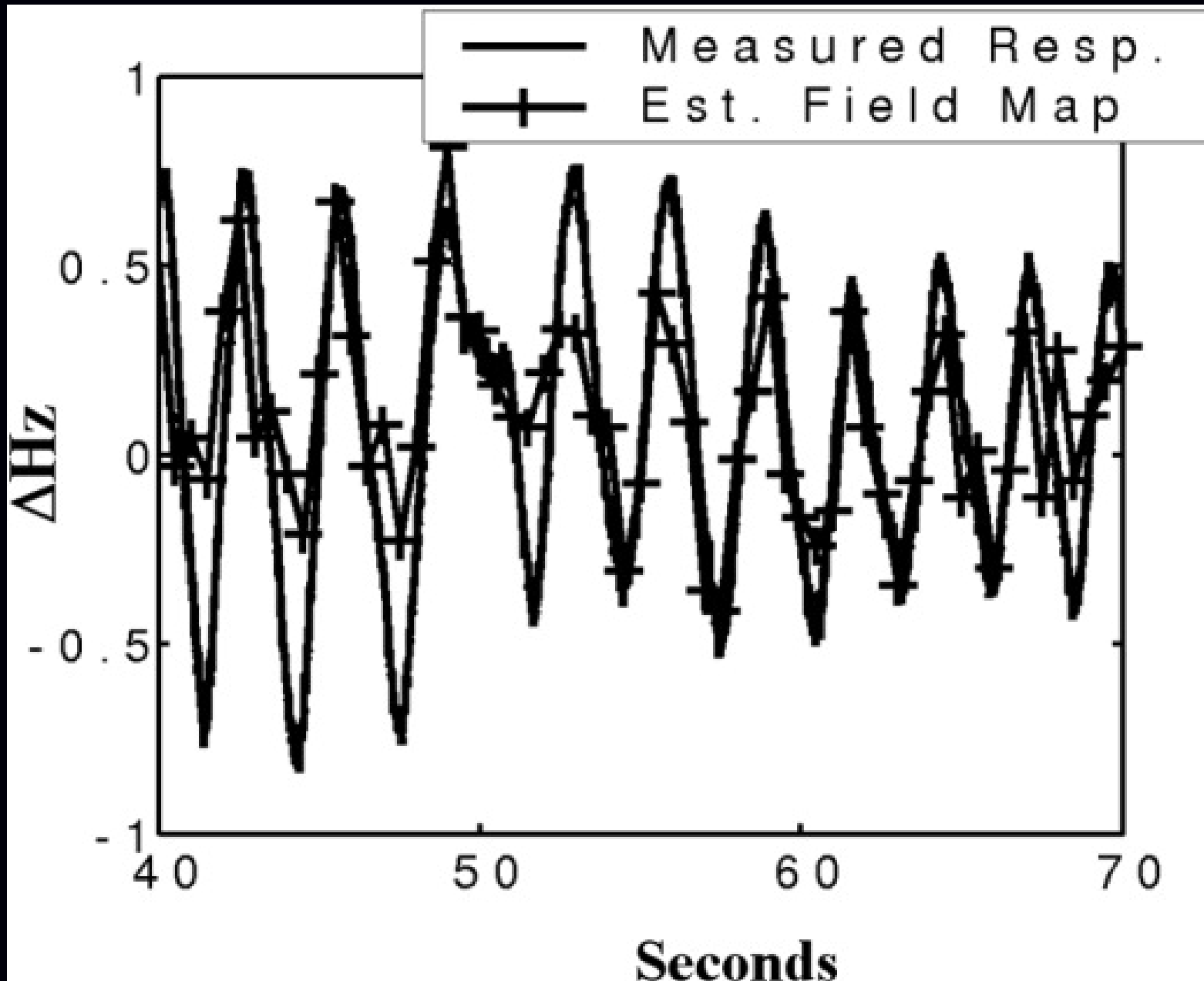
Reconstruction using the jointly estimated field map
for (d) subject 1, (e) subject 2, and (f) subject 3.

Number of pixels with correlation coefficients higher than thresholds
for (g) subject 1, (h) subject 2, and (i) subject 3.

Take home message: **dynamic field mapping is possible, using iterative reconstruction as an essential tool.**

(Standard field maps based on echo-time differences work poorly for spiral-in / spiral-out sequences due to phase discrepancies.)

Tracking Respiration-Induced Field Changes



Nonquadratic Regularization

Quadratic regularization is simple and reduces noise but impairs spatial resolution.

Nonquadratic regularization attempts to circumvent this tradeoff

Edge-preserving regularization has been investigated some for MRI:

$$R(f) = \sum_{j=2}^N \frac{1}{2} \psi(f_j - f_{j-1}),$$

where ψ rises less rapidly than a parabola, e.g., a hyperbola:

$$\psi(t) = \sqrt{1 + (t/\delta)^2}.$$

Challenges

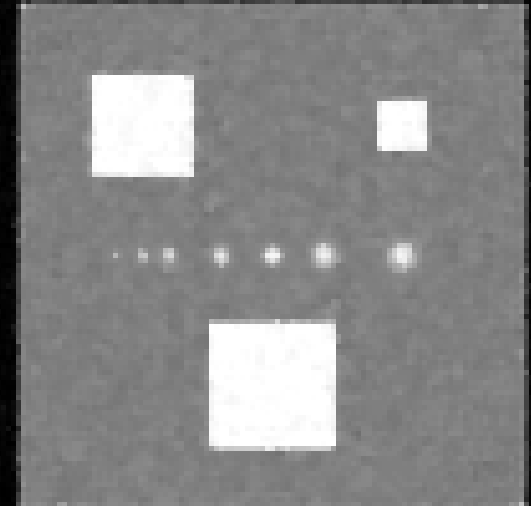
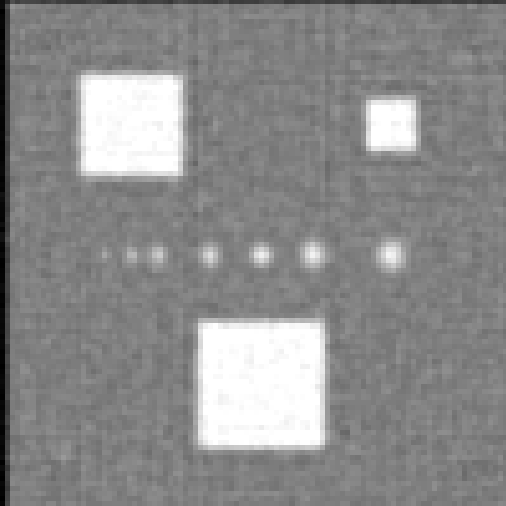
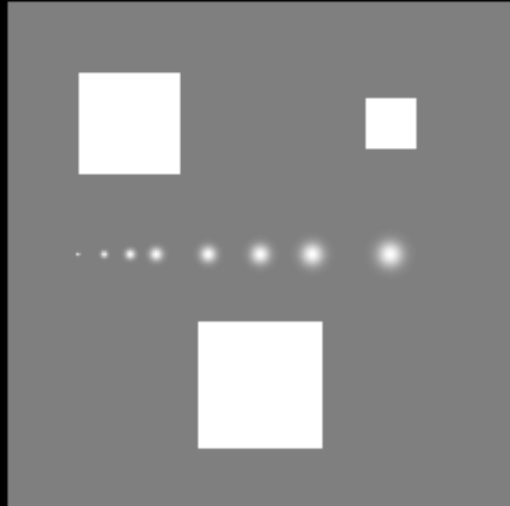
- choosing regularization parameter(s)
- characterizing nonlinear reconstruction results

Edge-Preserving Regularization Example

True

Quadratic

Edge-preserving

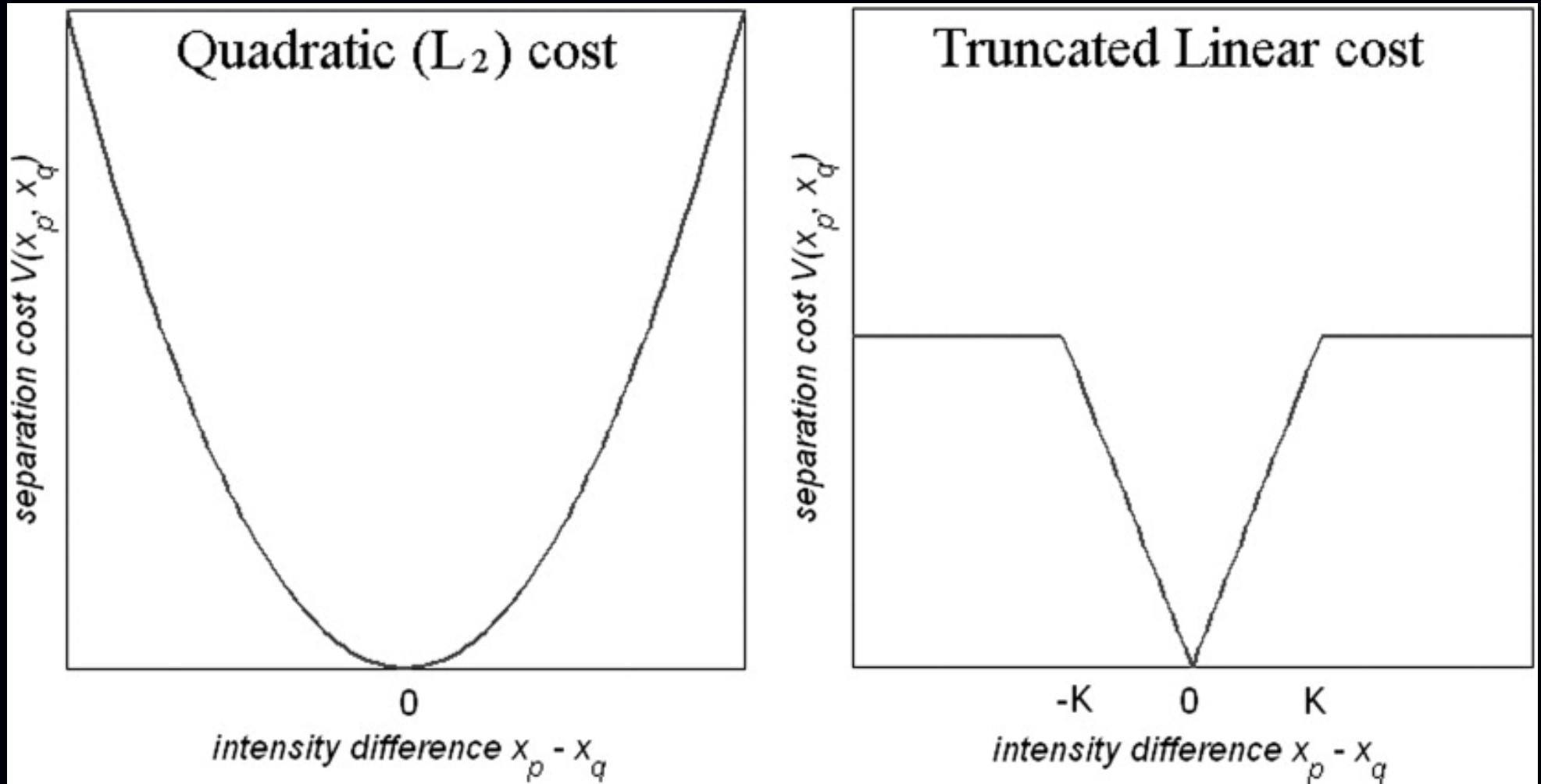


NRMS = 12.6%

NRMS = 11.0%

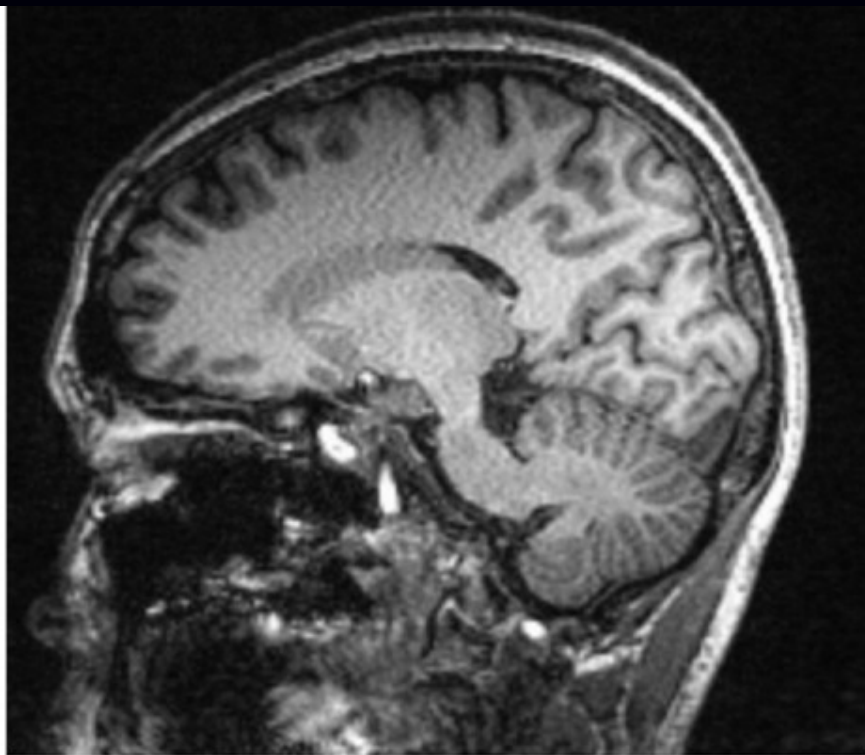
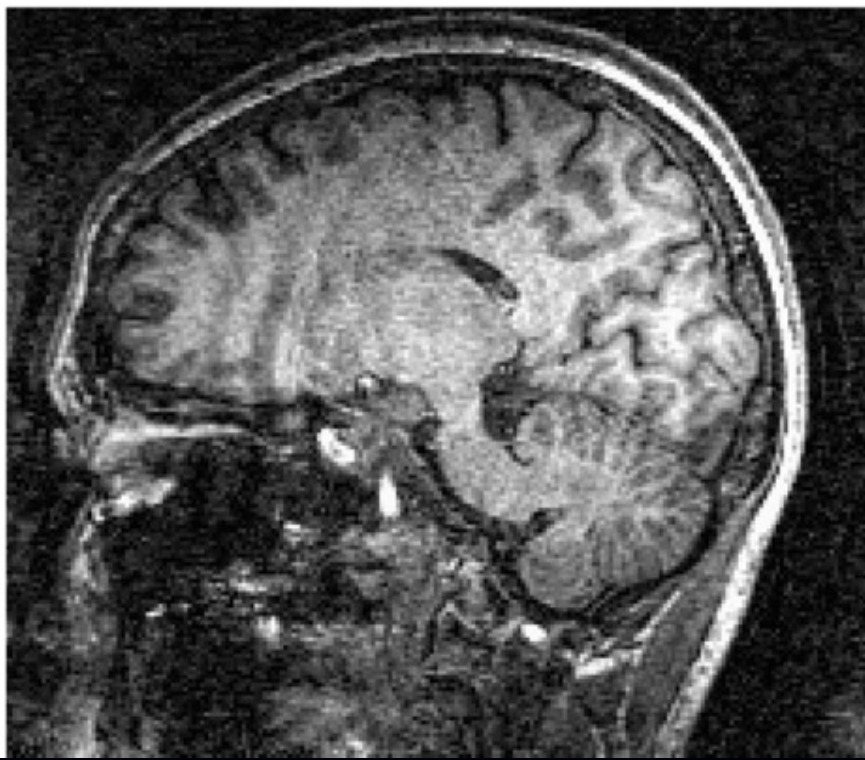
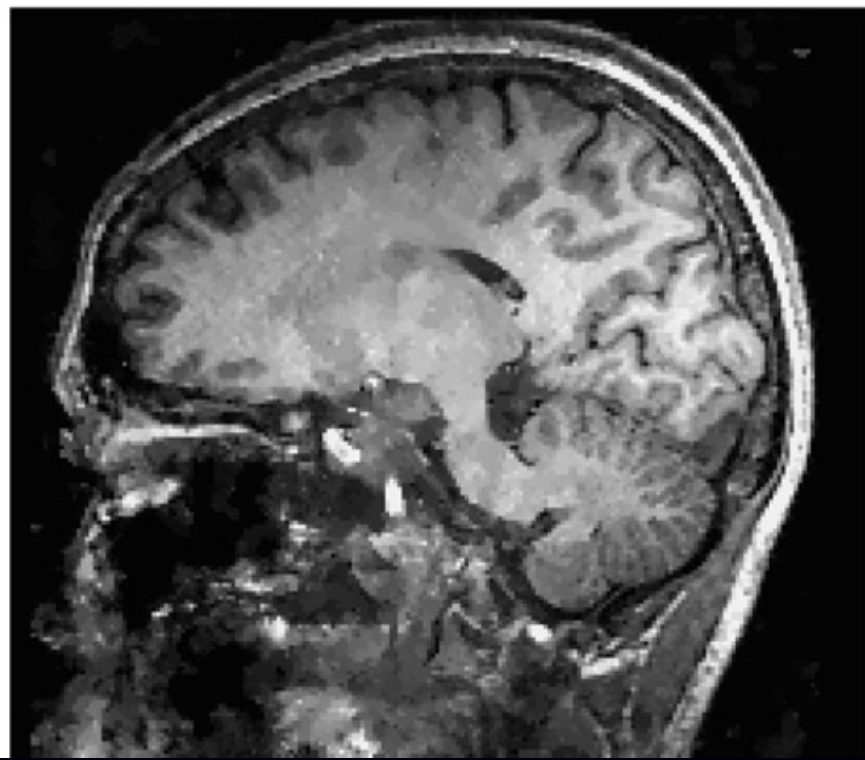
TV-like convex regularization

Nonconvex Edge-Preserving Regularization



Raj *et al.*, MRM, Jan. 2007

Applied to MR parallel imaging (multiple receive coils)

a**b****c****d**

Compressed sensing

(A form of nonquadratic regularization)

Find a transformation Ψ in which Ψf is (hopefully) **sparse**.

Sparsity regularization: $R(f) = \|\Psi f\|_0 = \sum 1_{\{[\Psi f]_k \neq 0\}}$

$$\text{or: } R(f) = \|\Psi f\|_1 = \sum_k |[\Psi f]_k| .$$

Compelling for under-sampled k-space data, e.g., dynamic scans.

Challenges

- optimization
- possibly multiple minimizers of $\|\mathbf{y} - \mathbf{A}f\|^2 + \beta \|\Psi f\|_1$
- choosing regularization parameter(s)
- characterizing nonlinear reconstruction results

(Very active research are in signal and image processing currently)

Sparsity

5%

10%

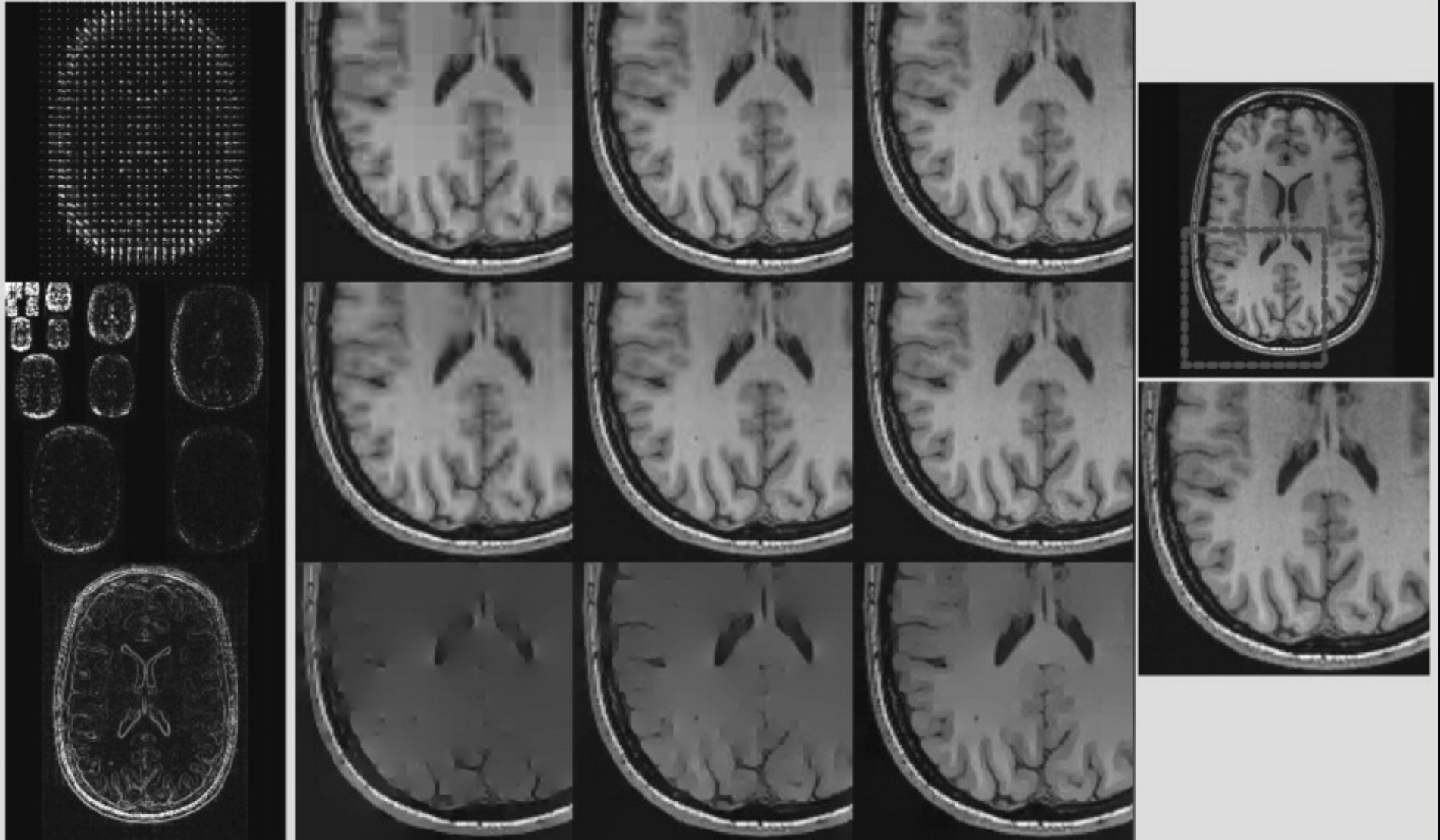
20%

100%

DCT

Wavelet

Finite diff.



Lustig *et al.*, MRM, Dec. 2007

Summary

- Model-based / iterative reconstruction: much potential in MRI
- Quadratic regularization parameter selection is tractable
- Computation: reduced by tools like NUFFT / Toeplitz
- But optimization algorithm design remains important (*cf.* Shepp and Vardi, 1982, PET)
- GPU: 100× acceleration (Haldar *et al.*, Hansen *et al.*, ISMRM 2008)
real-time interactive adjustment of regularization parameters

Some current challenges

- Nonquadratic regularization: analysis / design
Ahn and Leahy, IEEE T-MI, Mar. 2008
- Through-voxel field inhomogeneity gradients
- Motion / dynamics / partial k-space data
- Establishing diagnostic efficacy with clinical data...

OFF THE RECORD

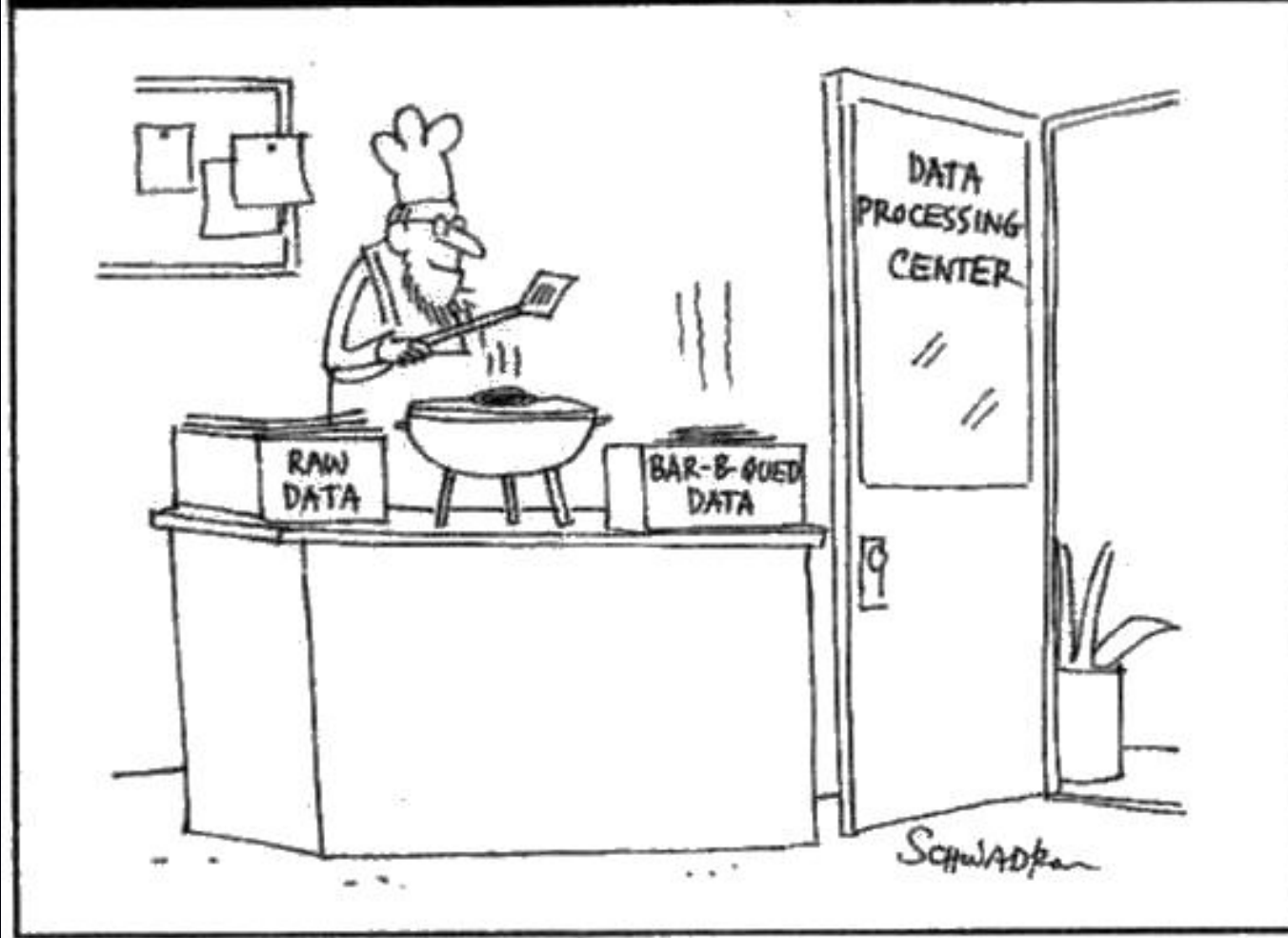


Image reconstruction toolbox:

<http://www.eecs.umich.edu/~fessler>